

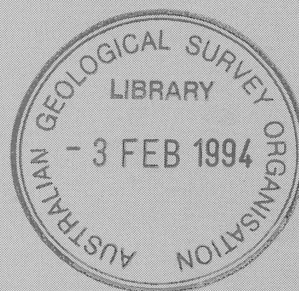
1994/2

C2

SEAFLOOR MORPHOLOGY AND TECTONICS OF THE CHRISTMAS ISLAND AREA, INDIAN OCEAN

BMR PUBLICATIONS COMPACTUS
(LENDING SECTION)

by
Irina Borissova



RECORD 1994/2



AGSO



AUSTRALIAN
GEOLOGICAL SURVEY
ORGANISATION

BMR COMP
1994/2
C2

AUSTRALIAN GEOLOGICAL SURVEY ORGANISATION

Department of Primary Industries & Energy

**SEAFLOOR MORPHOLOGY AND TECTONICS OF THE
CHRISTMAS ISLAND AREA, INDIAN OCEAN**

Irina Borissova

Division of Marine Geoscience and Petroleum Geology Program

Project 121.32

DEPARTMENT OF PRIMARY INDUSTRIES AND ENERGY

Minister for Resources: Hon. David Beddall, MP

Secretary: Greg Taylor

AUSTRALIAN GEOLOGICAL SURVEY ORGANISATION

Executive Director: Harvey Jacka

© Commonwealth of Australia

ISSN: 1039-0073

ISBN: 0 642 20092 0

This work is copyright. Apart from any fair dealings for the purposes of study, research, criticism or review, as permitted under the Copyright Act, no part may be reproduced by any process without written permission. Copyright is the responsibility of the Executive Director, Australian Geological Survey Organisation. Inquiries should be directed to the **Principal Information Officer, Australian Geological Survey Organisation, GPO Box 378, Canberra City, ACT, 2601.**

CONTENTS

	Page
INTRODUCTION	1
DATA PROCESSING AND BATHYMETRY MAP COMPILATION	2
Collecting and formatting the data	2
Gridding and contouring	5
Editing of contours	7
Compilation of overlay maps	8
COMPILATION OF A SEDIMENTARY THICKNESS MAP	9
SEAFLOOR MORPHOLOGY AND TECTONICS IN THE CHRISTMAS ISLAND AREA	10
The Java Trench	11
The fore-arc ridge	14
Fore-arc basins	15
The Northeastern Wharton Basin in the Christmas Island region	16
Plate tectonics of the Christmas Island area	18
Seamount age and origin	20
CONCLUSIONS	22
REFERENCES	23

FIGURES

1. The GEBCO map bathymetry of the Christmas Island area. Contour interval 500 m.
2. Contours from the new ORMS map. Contour interval 400 m.
3. Data points digitised from GEBCO "collector" sheets.
4. Tracklines of surveys which provided digital records of water depths (NGDC and AGSO data) for the new bathymetric map. Points - the same as on the Fig. 3.
5. An example of gridding and contouring of irregularly spaced data with the Petroseis version 7 algorithm (minimum curvature surface fit).
6. Results of gridding and contouring with the CPS Radian program. The same test area as on the Fig. 5.
7. Results of interactive editing of the contours presented on the Fig. 6.
8. Location of geological stations in the Christmas Island area. Bathymetry is shown with a 1000 m interval.
9. Locations of the dredge sites.
10. Locations of the core sampling.
11. Location of the free-fall gravity grab sites.
12. Tracklines of the seismic surveys in the Christmas Island area.
13. The sedimentary thickness map. Isopach map in 200 m contours; bathymetry - faint colour 1000 m contours.
14. Large shallow earthquakes ($M_s > 7.0$; $z < 70$ km) of this century are plotted with year beside the epicentral location (after Newcomb and McCann, 1987).
15. Location of the study area in its geodynamic setting (modified from Moore et al., 1980).

16. Single-channel analog seismic reflection profiles across the Sunda Trench
a) in the Java province at about 110° E (Scripps Oceanographic Institute, Eurydice expedition); b) in the South Sumatra province at about 103° E (Lamont-Doherty Geological Observatory, Conrad 14)
17. Example from Aleutian Trench (from Scholl et al., 1982) illustrating changes in the basement structure at the intersection with a large former transform fault:
a) magnetic lineations displaced by the Amliia fracture zone; b) contours of the trench basement in km.
18. Tectonic map of the Christmas Island area.
19. Interpretation of Gloria images (a) and original sonographs showing seamounts at different stages of collision with accretionary wedge (b) early stage; (c) advanced stage (after Masson, 1990).
20. A. SeaMARC II bathymetry of the eastern termination of the Java Trench; a seamount colliding with the accretionary wedge (after Breen et al., 1986). B. Single-channel seismic section across the northern edge of the seamount shown above (after Milsom et al., 1992).
21. Extensional structures in Sunda strait on the continuation of Sumatra fault system (after Lassal et al., 1989)
22. Observed and inferred seafloor spreading isochrons. Predicted position of the extinct spreading axis abandoned 96 Ma ago (after Powell et al., 1988).
23. Hypothetical plate boundaries in the Tethys during Mesozoic and Cenozoic (after Scotese et al., 1988): a) Early Cretaceous; b) Middle Cretaceous; c) Cretaceous Magnetic Quiet Zone; d) Late Cretaceous; e) Paleocene; f) Oligocene.
24. Detailed bathymetry of Christmas Island.

TABLES

1. Surveys with analog bathymetry used in GEBCO map compilation.
2. Surveys with digital bathymetry from NGDC data bank used for the ORMS map compilation.
3. Surveys with seismic reflection profiling used for compilation of the sedimentary thickness map.

INTRODUCTION

Christmas Island lies about 1600 km north-north west of Australia's Northwest Cape and approximately 350 km south of Java in the northern part of the Wharton basin (Indian Ocean). Recently Australia declared a 200 mile Fisheries Zone around the island and AGSO was asked to assess seabed morphology, sediment thickness and offshore mineral resources in this area. In February 1992 R/V "Rig Seismic" carried out a detailed survey of the region, providing relevant data for the required assessment. Eight seismic profiles were acquired on this cruise, totalling about 2000 km, and almost twice as much bathymetric data was recorded. In conjunction with seismic and bathymetric data collected by other institutions, our data provides a good coverage of the area, which enabled us to compile a new bathymetric map and to produce the first sediment thickness map.

Among the published bathymetric maps only three cover the Christmas Island area: 1) published by Udintsev (Geophysical Atlas of the Indian Ocean, 1975; 1:5,000 000), 2) by Mammerickx et al. (1976, 1:5,000 000) and 3) 1:10,000 000 General Bathymetric Compilation (GEBCO) map, published by the International Oceanographic Service (1982). All published bathymetric maps were compiled in the end of the 1970s and the beginning of the 1980s, and all of them were based on processing analog records of water depths and were drafted manually. Moreover, most of the data for map compilation were collected using a sextant, and only a very limited using satellite navigation.

The amount and quality of data collected by the end of the 1970s allowed the production of the fairly accurate 1:5,000 000 and 1:10,000 000 maps of the Indian Ocean listed above, however a lot of smaller features, such as individual seamounts, are missing on those maps. Insufficient data coverage led to broad extrapolation of bathymetric trends, sometimes derived purely from magnetic lineation pattern (Fig.1). To the east of Christmas Island the lack of information is particularly evident: all the maps differ in their interpretation of this area.

New high quality data collected by "Rig Seismic", and digital water depths obtained from the USA National Geophysical Data Bank (NGDC), were used for compilation of a new revised version of the bathymetric map on the Christmas Island area in a 1:1,000 000 scale. The new map (to be published in AGSO's Offshore Resources Map Series) contains a lot more detail on the complex bathymetry of the area, and gives a more realistic picture of seamount distribution and the structure of the Java Trench and Java's outer-arc ridge. The amount of added information can be clearly deduced from comparison of Fig.1 and Fig.2. The time scale used in this report is that of McDougall (1974) and Falloon et al. (1993).

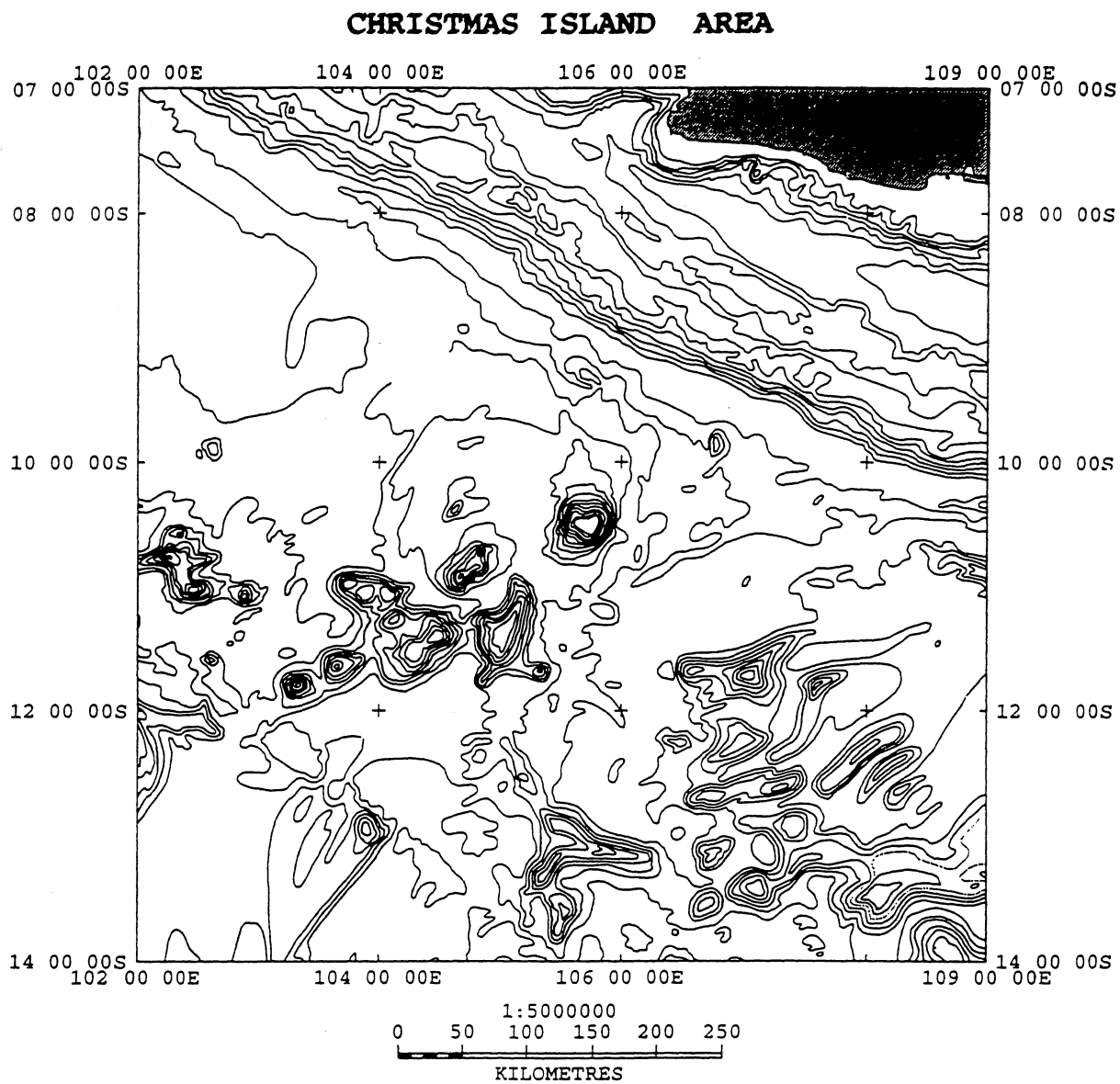


Fig. 1. The GEBCO map bathymetry of the Christmas Island area. Contour interval 500 m.

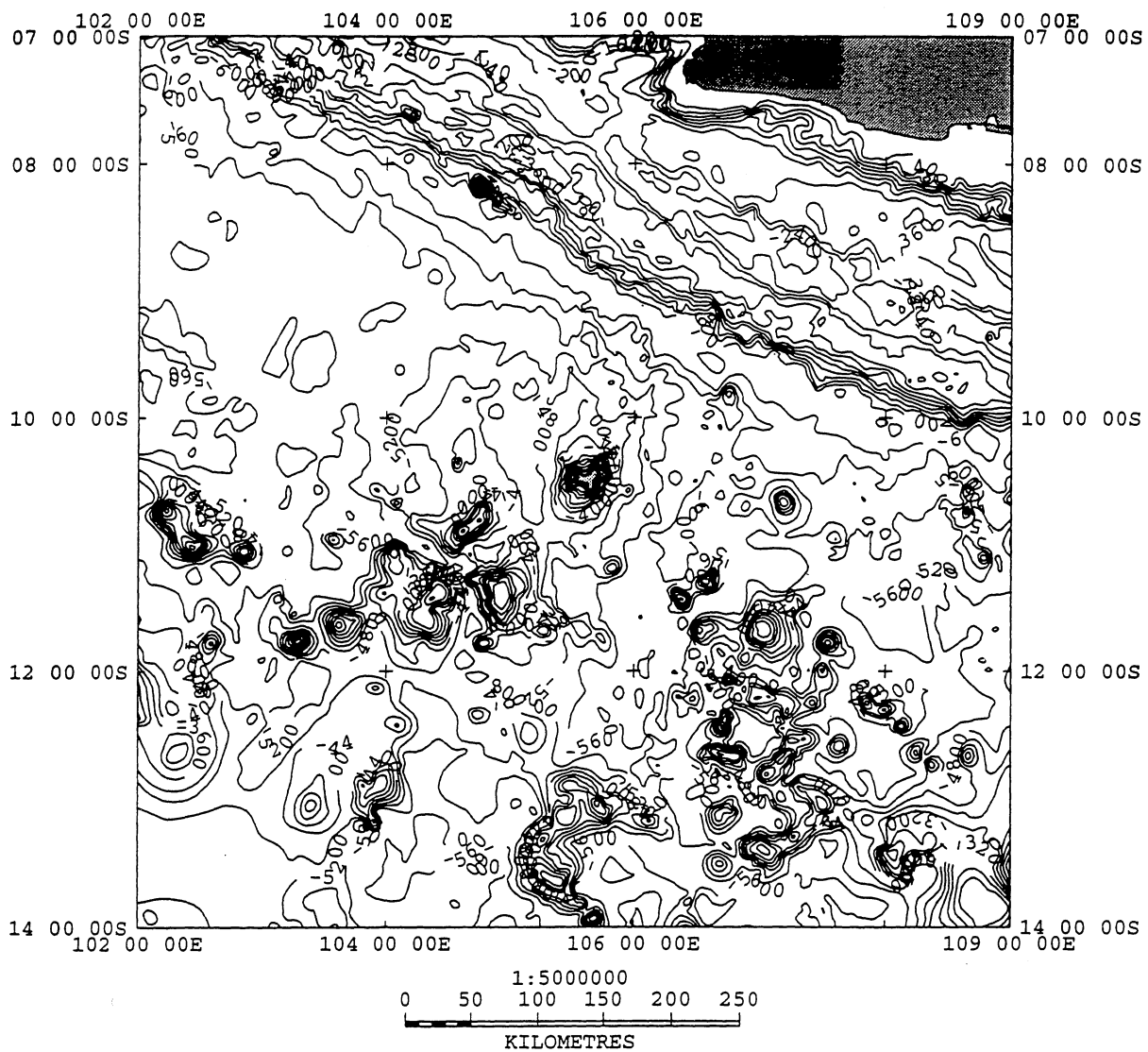


Fig. 2. Contours from the new ORMS map. Contour interval 400 m.

Acknowledgments

This work benefited greatly from discussions with Neville Exon, Phil Symonds and Chao-Shing Lee. I want to particularly thank Neville Exon, whose thorough and careful review has helped to clarify and improve the report.

I would like thank all those who contributed to the successful completion of this work:

Peter Petkovic for preparing water depths from the "Rig Seismic" survey and from files from the NGDC data bank, Ian Roach for making corrections to the "Rig Seismic" water depths, and Jenny Bedford for assistance with Petroseis software throughout the project.

My special thanks are due to Mike Sexton for his valuable assistance in managing differently formatted data, testing gridding and contouring algorithms, and dealing with other technical problems on all stages of the project.

DATA PROCESSING AND BATHYMETRY MAP COMPILATION.

The process of bathymetric map compilation involved several stages:

1. Collecting and formatting the data
2. Data processing - gridding and contouring
3. Editing of the contours
4. Compilation of overlay maps: a) track lines of different surveys;
b) geological stations

1 Collecting and formatting the data

Originally there were 4 sources of data:

1. digital water depths from the "Rig Seismic" survey;
2. digital water depths from the US National Geophysical Data Centre (NGDC);
3. unpublished 1:100000 map around the Christmas Island compiled by the Australian Hydrographic Office;
4. GEBCO "collector" sheets (1:1000000), with manually plotted water depth values.

The first and the most time-consuming stage of the map compilation was associated with converting all non-digital data (3 and 4) into digital format. Water depth values from the GEBCO sheets (Fig. 3) were digitised in sequences corresponding to individual surveys (identified from the charts of the tracklines). A list of surveys whose data was put into the

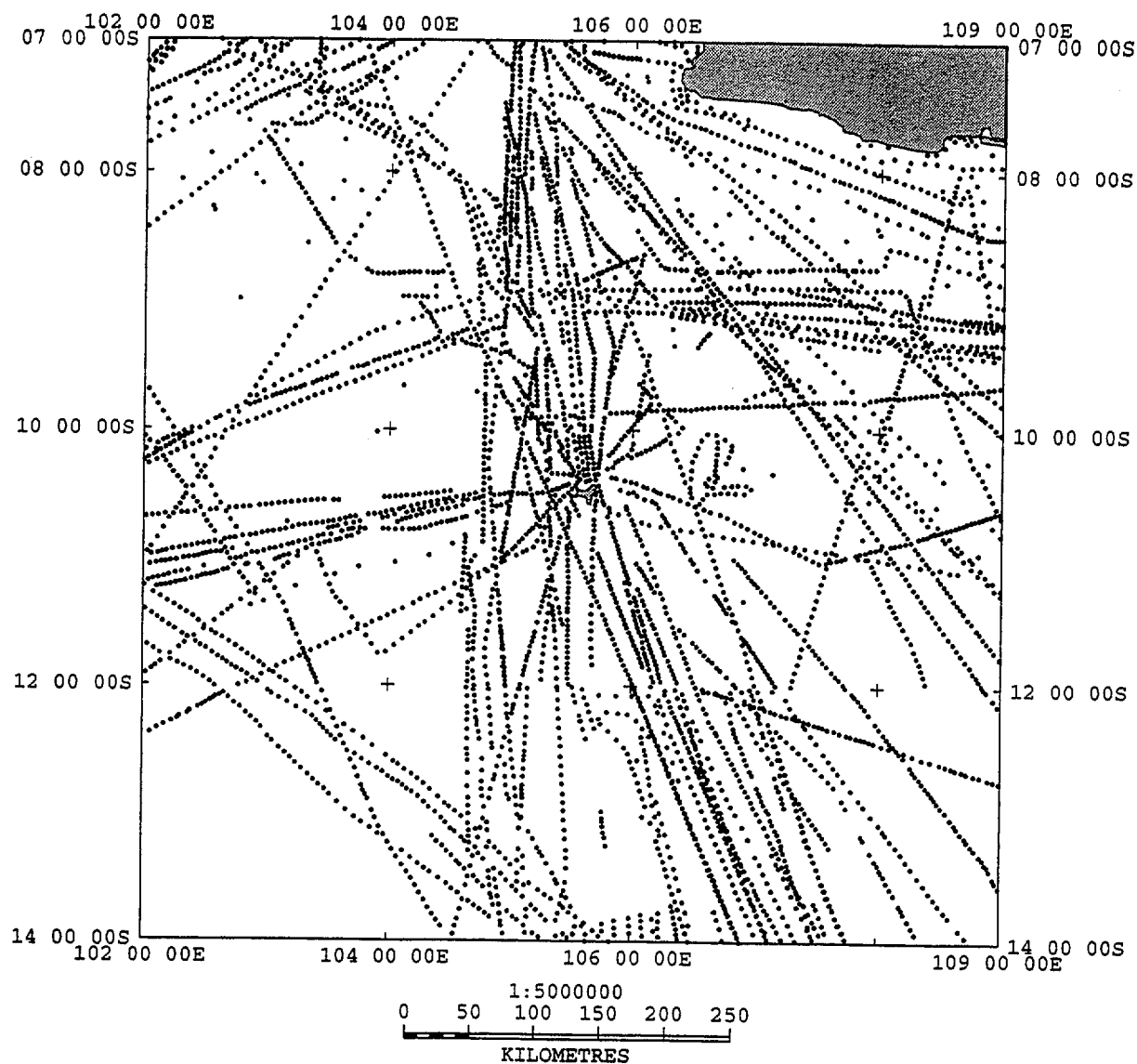


Fig. 3. Data points digitised from GEBCO "collector" sheets.

database is presented in Table 1. Water depths were initially stored in the cultural database of Petroseis, but later it was decided to import them into a seismic master file for the convenience of displaying seafloor profiles, which is not possible in the cultural database. The Christmas Island large-scale map (3) was digitised as a Petroseis contour file, which enabled us to use it directly for gridding and contouring procedures.

Table 1. Surveys with analog bathymetry used in GEBCO map compilation.

COUNTRY	PLATFORM	YEAR
AUSTRALIA	DIAMANTINA	1960 1962 1963 1964
		1966 1968 1971 1972
		1974 1975 1976 1979
	COOK	1985 1990
	GASCOYNE	1962 1963
	MORESBY	1965 1968 1983 1985
	DAMPIER	1967
	VENDETTA	1961
	SCARBOROUGH	1959
	DEWENT	1972
USA	VEMA	1963 1964 1967
	ARGO	1960 1962
	VOYAGER	1960
	HORIZON	1962
	BARTLETT	1971
UK	HYDRA	1973
USSR	VITALAZ	1959 1960 1960-61
		1962
OTHER COUNTRIES	ENTERPRISE	1967
	INVINCIBLE	1983-84
	STUART	1972

Digital bathymetric data for the Christmas Island area extracted from the NGDC files (Fig. 4) was contained in two formats: as water depths, assuming a certain sound velocity or as two-way travel time. We used Matthew's Tables to work out proper corrections for sound velocity in the region. Because our area of interest is fairly small it falls within one zone of similar water properties, where average sound velocity is about 1500 m/s, the value which we used for all our data. All the water depths that were calculated with different sound velocity values were recomputed and the data contained in travel-time units was converted into water depths. Then all files were reformatted into UKOOA format and imported into the Petroseis seismic master file. Brief information about the surveys with digital data which were used for the map compilation is contained in Table 2.

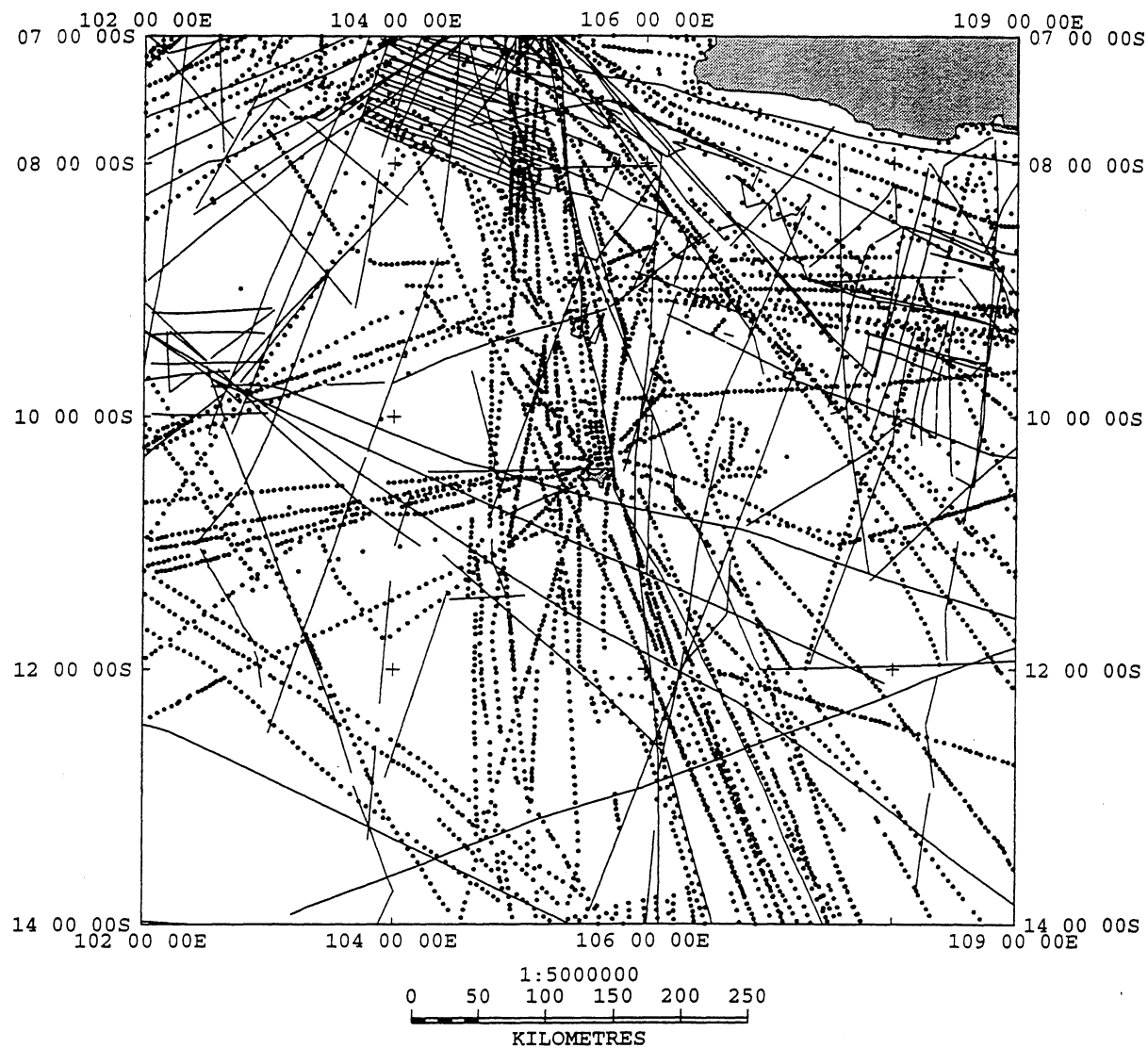


Fig. 4. Tracklines of surveys which provided digital records of water depths (NGDC and AGSO data) for the new bathymetric map. Points - the same as on the fig. 3.
I - boundaries of the test area (Fig. 5,6,7)

Table 2. Surveys with digital bathymetry from NGDC data bank used for the ORMS map compilation.

COUNTRY	INSTITUTION	PLATFORM	PROJECT	YEAR	INITIAL FORM OF DATA	SAMPLING INTERVAL (MIN)
USA	LAMONT-DOHERTY GEOLOGICAL OBSERVATORY	R. CONRAD	CRUISE 14, LEG. 3	1971	ANALOG RECORDS	6
		R. CONRAD	CRUISE 2703	1986	DIGITAL	5.3
		VEMA	CRUISE 19, LEG. 9	1963	ANALOG RECORDS	6
		VEMA	CRUISE 28, LEG. 19	1971	ANALOG RECORDS	6
		VEMA	CRUISE 29, LEG. 1	1971	ANALOG RECORDS	6
		VEMA	CRUISE 24, LEG. 10	1967	ANALOG RECORDS	6
	WOODS HOLE OCEANOGRAPHIC INSTITUTION	CHAIN		1971	ANALOG RECORDS	5
		ATLANTIS II	CRUISE 93, LEG. 14	1976	ANALOG RECORDS	5
	NAVAL OCEANOGRAPHIC OFFICE	USNS WILKES	NAVOCEANO, LEG. 18, 20	1978	DIGITAL	1
		USNS WILKES	NAVOCEANO, LEG. 17, 20	1978	DIGITAL	1
		USNS WILKES	NAVOCEANO, LEG. 27, 10, 9	1978	DIGITAL	1
	SCRIPPS INSTITUTION OF OCEANOGRAPHY	ARGO	DODO, LEG. 9	1964	ANALOG RECORDS	6
		ARGO	LUSIAD, LEG. 6C	1962	ANALOG RECORDS	6
		ARGO	LUSIAD, LEG. 6D	1962	ANALOG RECORDS	6
		ARGO	LUSIAD, LEG. 6E	1963	ANALOG RECORDS	6
	SCRIPPS INSTITUTION OF OCEANOGRAPHY	MELVILLE	ANTIPODE, LEG. 5	1970	ANALOG RECORDS	5
		TH. WASHINGTON	INDOPAC, LEG. 14	1977	ANALOG RECORDS	5
		TH. WASHINGTON	RAMA, LEG. 5	1980	ANALOG RECORDS	5
		GLOMAR CHALLENGER	DSDP, LEG. 22	1972	ANALOG RECORDS	5
		HORIZON	LEG. 3	1962	ANALOG RECORDS	5
	TEXAS UNIVERSITY	JOIDES RESOLUTION	ODP, LEG. 122	1988	DIGITAL	5
		JOIDES RESOLUTION	ODP, LEG. 123	1988	DIGITAL	5
USSR	VNIIGEOPHYSICS AN USSR	DM. MENDELEEV	LEG. 7	1971-72	ANALOG RECORDS	10
	IFZ AN USSR	DM. MENDELEEV	LEG. 10	1973	ANALOG RECORDS	10
FRANCE	IFREMER	JEAN CHARCOT	KRAKATAU 85	1985	DIGITAL	1.2
NEW CALEDONIA	GEOMER DATA BANK FORSTOM	CORIOLIS	COR900	1983	ANALOG RECORDS	5
		CORIOLIS	GIN100	1984	ANALOG RECORDS	5
JAPAN	UNIVERSITY OF TOKYO	HAKUHO MARU		1972	ANALOG RECORDS	12
		HAKUHO MARU		1976-77	ANALOG RECORDS	9.3
		UMITAKA MARU	CRUISE 1969	1969-70	ANALOG RECORDS	10

The imported data were displayed and checked, both for location and by scanning water depth profiles, to ensure data consistency. Water depths from the "Rig Seismic" survey were processed in a similar way and also imported into the seismic master file.

2. Gridding and contouring

The next stage was gridding and contouring of the data. The Christmas Island map is one of the Offshore Resource Series Maps (ORMS). Maps of this series cover the Australian continental margin. All maps are compiled at 1:1,000,000 scale and their compilation essentially is based mostly on BMR survey data. Compilation of this particular map sheet was different in many aspects. First, this area remote from Australian margin has not been explored to the same extent as areas close to the continent. Second, being far from coast, navigation of the earlier surveys was never as good as in the coastal areas where onshore features could be used for control. These two circumstances required the use of all available data, even if they are old and not very accurate and, at the same time, techniques to handle inconsistencies between the data collected at different times by different institutions.

At the start of the ORMS project, in order to work out a standard procedure for compilation of all subsequent maps, a number of gridding and contouring algorithms were tested by C. Johnston in 1990. It was shown that irregularly spaced data (in our case ship tracks) makes automatic machine contouring very difficult and contour distortions are produced by all algorithms. However, in respect of ORMS map data sets, a distance weighted algorithm of Petroseis version 6 produces the most realistic contours. In this method, the weighting used is inversely proportional to the square of the distance between the grid point and the data point. The search radius about each grid point was 50 km and the sampling distance 5 km. This algorithm was preferred to the others, because it copes better with the abrupt changes of gradient common for topography, and the number of artificial highs and lows produced by the system is significantly less in comparison to other algorithms.

In Petroseis version 7, currently installed at AGSO, there is no choice of gridding techniques. The gridding procedure built into the program uses a series of gridding passes, each of which results in a grid cell size that is half of the size of the previous grid cell size. Within one grid cell, grid values are estimated using a projected distance weighted average technique, using slope information derived from previous gridding passes and, for more distant grid nodes, values are computed using an algorithm that minimises the net surface curvature. The contouring technique is fairly straightforward and the results of contouring are fully dependent on the input grid. To trace contour lines through a grid cell, the system first subdivides the grid cell into a series of subgrid cells. The number of subgrid cells is defined by the user. Contours are then traced through these subgrids as straight lines within a triangular subdivision of each cell.

According to the previous assessment by C. Johnston (1990) the minimum curvature algorithm gives very good results for contouring of magnetic or gravity fields, but smooths too much and creates artificially low-angle broad slopes, when applied to topography. At the same time when assessment of algorithms took place, the number of data points that could be processed within the program was limited. Therefore, original data were resampled at a 5 km interval, and with this sparse sampling the distance weighted algorithm showed the best results. The new system can process a huge number of data points and although the problem of large gaps between the track lines remains, we decided to explore the possibilities of the system to use as much data as possible for gridding and contouring, varying gridding parameters.

A series of maps (one of them is shown in Fig.5) was produced for a test area (Fig.4), within which spacing between the ship tracks varies considerably: it is rather dense in the west and sparse in the east. Results of our tests show that, with the gridding algorithm of the Petroseis version 7, it is possible to produce a bathymetric map of reasonable quality for areas with a dense survey coverage (average spacing between the track lines about 10-15 km). An appropriate sampling interval for an accurate map is 1500-2000 m. In the Christmas Island area the data coverage is very irregular: in some areas the distance between the track lines doesn't exceed 5 km (Sunda Strait), in others is more than 50 km. In the areas of sparse data distribution, gridding techniques fail to produce anything reasonable, the slopes of seamounts are stretched enormously (for instance, the large seamount in the north-west part of the test area) and artificial highs and deeps are created. The only possibility to compile a realistic bathymetric map with these techniques is to limit the search radius to 20-25 km (basically limit the extent of extrapolation), and to draw the contours in between manually, using geologic expertise.

Another option was to use a different software product. We settled our choice on a comprehensive gridding and contouring package produced by the Radian Corporation (CPS-3). A completely new approach, convergent gridding, is used in the program. It starts with a coarse grid spacing and converges to a fine spacing, hence the name "convergent gridding". The convergent gridding approach doesn't require a post-processing step, because smoothing and control point tying is imbedded in the process. In each iteration a finer grid is produced, built upon the previous iteration, and at each step the grid both honours the raw data and is as smooth as the control point honouring allows. Because raw data values, slopes and curvature are an integral part of each step of the convergent gridding algorithm, artefacts, which are difficult to trace and remove with traditional post-processing smoothing and tying algorithms, are prevented from being introduced into the

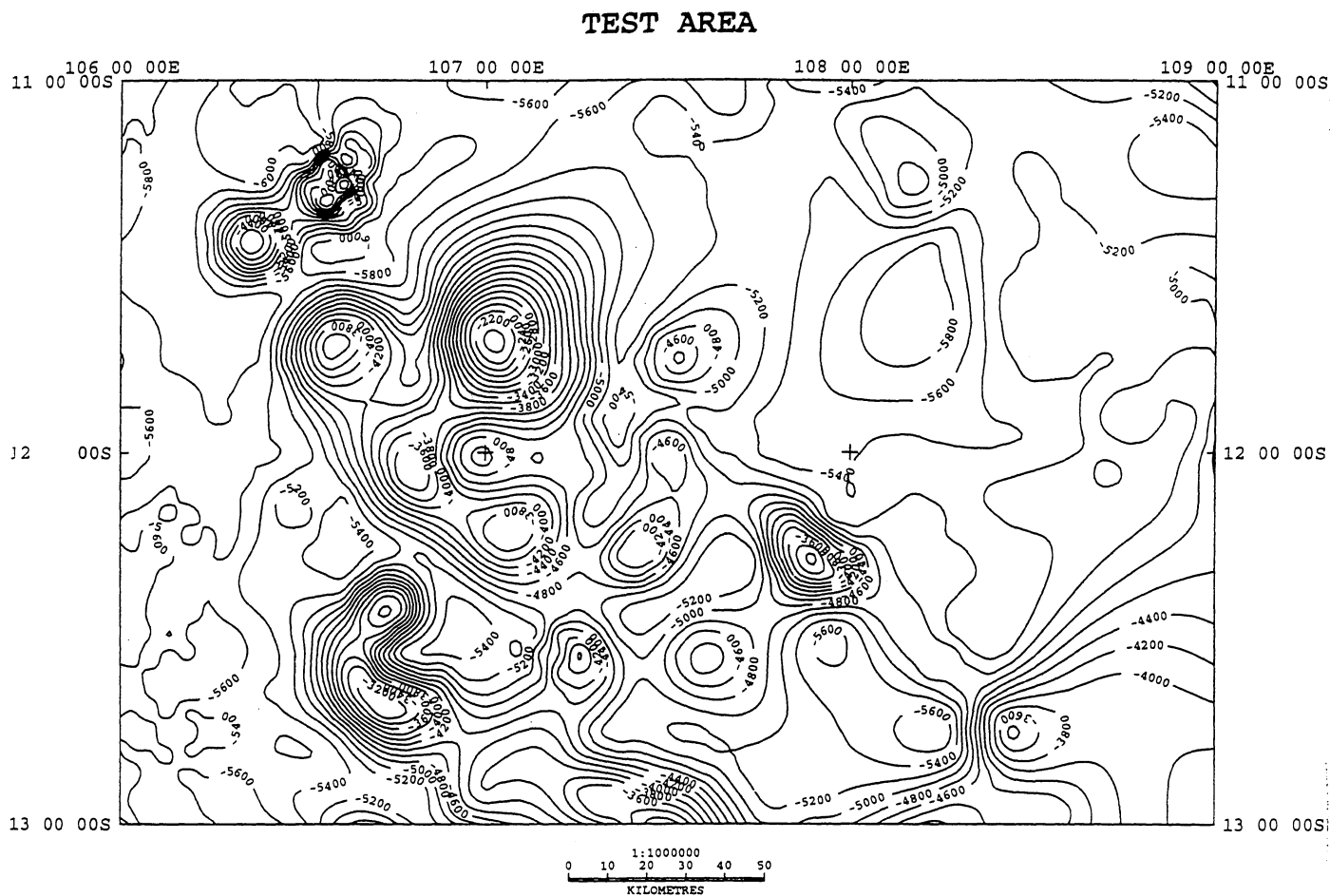


Fig. 5. An example of gridding and contouring of irregularly spaced data with the Petroseis version 7 algorithm (minimum curvature surface fit).

resultant grid. Radian corporation tested the algorithm on bathymetric data and presented very good results (M.A. Haecker, 1992).

We processed our data using the CPS-3 Radian program and compared the resultant map (Fig.6) with the one, produced using Petroseis (version 7). Comparison of the two maps (Figs.5 & 6) shows clearly that the CPS Radian program is a much more appropriate product for compilation of bathymetric maps. Contours produced by this program are tied very well to raw data and the map shows much more detail and complexity in the seafloor topography. At the same time this algorithm is also incapable of producing a "perfect" map. Honouring the data means sometimes that inconsistencies in water depths between adjacent or intersecting tracklines may result in artefacts. Moreover, the data set digitised from the GEBCO sheets includes isolated data points. When one of these data points occurs at a considerable distance from the trackline and its value differs from those on the tracklines, the program draws the whole set of contours, creating an unjustified high or a deep around this data point. Therefore, although we were generally satisfied with the results of gridding and contouring with CPS radian, it was still necessary to edit the computer produced map.

3. Editing of the contours

An important stage of map preparation is checking and editing of the computer produced map. The Petroseis software (version 7) allows one to make all checking and corrections interactively on the screen. There are certain difficulties in working in an interactive regime with large files, contour file for the whole map sheet in our case. Making a local copy of a large file and saving changes takes a very long time. Moreover, a full-screen image of the file is displayed at a very small scale, which is limited by the size of the monitor, and it is necessary to use multiple zoom in function in order to get the right scale. To counter this difficulty the Christmas Island map sheet was divided into 6 subsheets and edited using geologic expertise. Editing procedures involved:

1. Displaying posted values of water depths along all ship tracks with a minimum possible increment (3-5 km);
2. Open editing of the contour file;
3. Checking whether all local highs and deeps are justified by the raw data and if not, deleting those features;
4. Identifying and deleting small isolated contours that don't affect the general distribution of depths;
5. Identifying areas with large spacing between the tracks, critically reviewing the computer interpretation, and making necessary corrections;

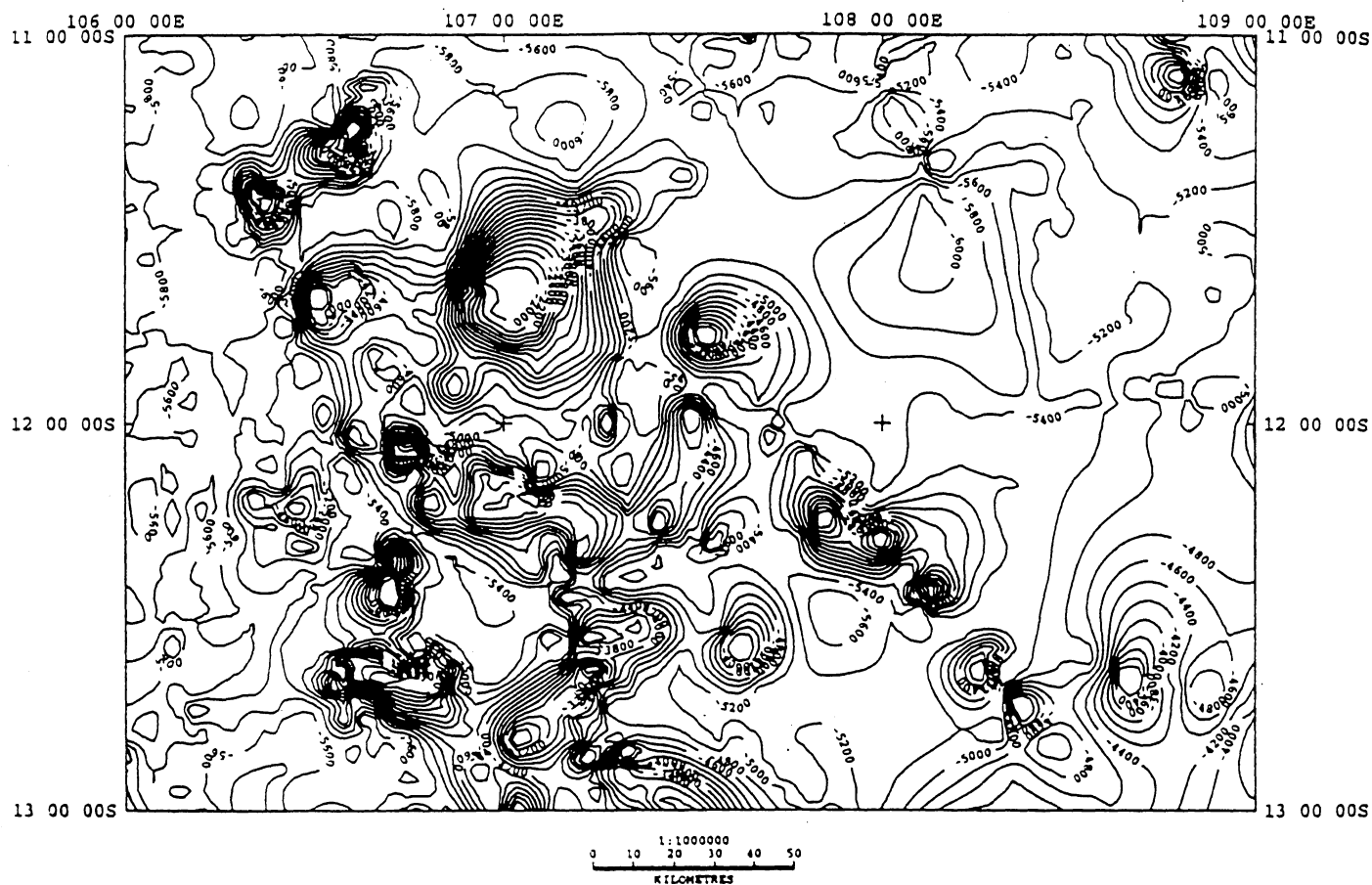


Fig. 6. Results of gridding and contouring with the CPS Radian program. The same test area as on the Fig.5.

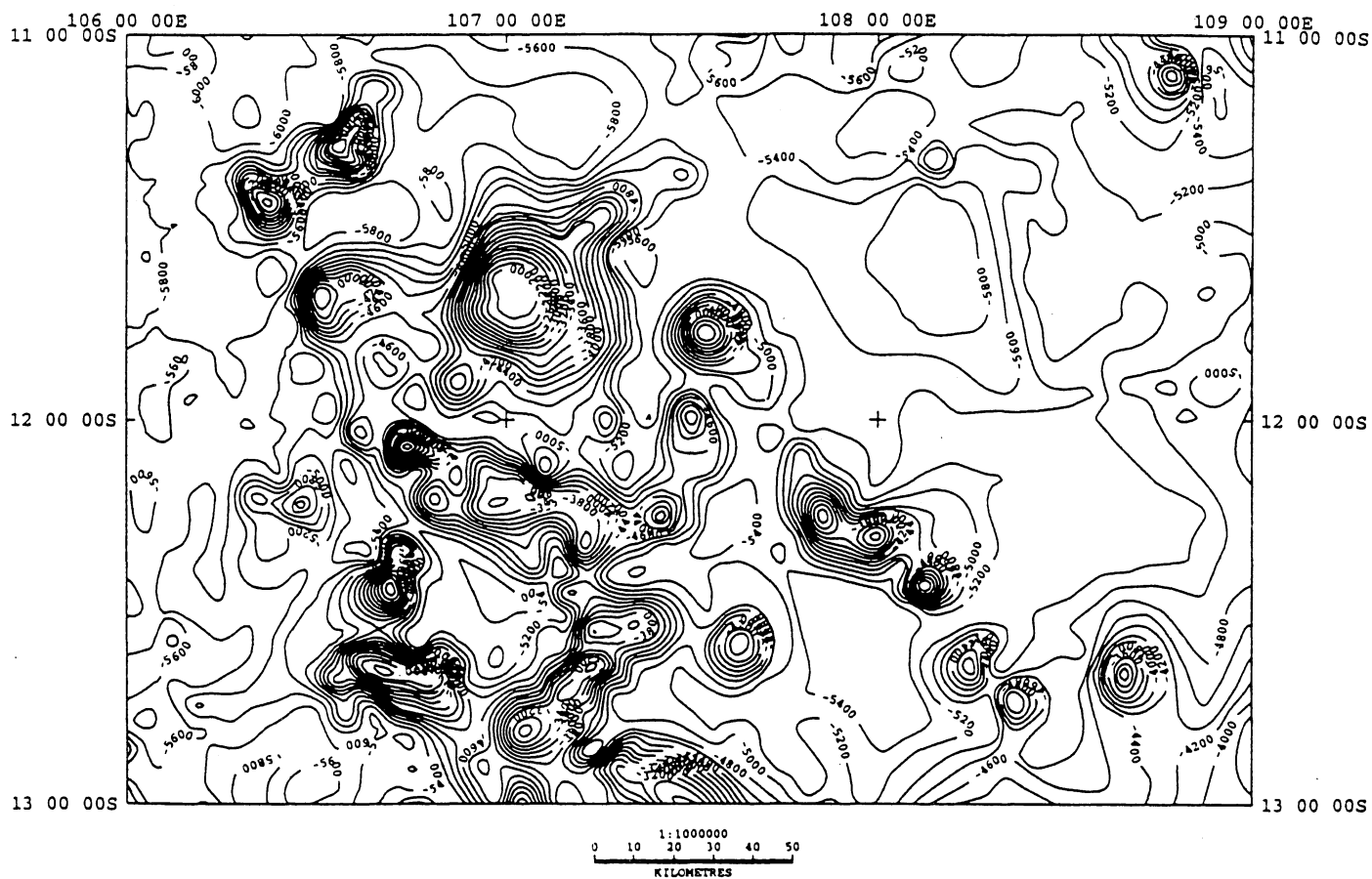


Fig. 7. Results of interactive editing of the contours presented on the Fig.6.

6. Checking seamount slopes, identifying broad uniform slopes unjustified by data, not very well drawn saddles and troughs dissecting seamount slopes and making relevant changes.

An edited version of the test area map is presented in Fig.7. Comparing it with the computer produced version (Fig.6) gives an idea about the nature and number of corrections that were made in the course of final map preparation.

At the editing stage a decision about changing contour interval was made. The previous ORMS maps were compiled with a 100 m interval, and on some map sheets within areas poorly covered by data a 500 m interval was used. In our case the quality and distribution of data are not very favourable and the root mean square error in gridding and contouring amounted to slightly more than 100 m. Therefore it was unreasonable to stay with the 100 m interval. Moreover, seamounts and ridges with steep slopes are abundant in the area, and spacing between 100 m contours on such slopes would be less than the map resolution allows. Taking into account these two facts, it was decided to produce the whole map with a 200 m interval.

4. Compilation of overlay maps.

Apart from colour-filled contour intervals, ORMS maps contain information about data distribution and location of geological sampling sites. Two overlay maps were prepared :1) a map of data points, used in the map compilation, and 2) a map of geological sites.

All data points digitised from the GEBCO sheets are shown with individual symbols on the first map. It was not possible to show all data points that were used for gridding and contouring from NGDC and "Rig Seismic" surveys because of their extremely dense distribution. the algorithm used for the previous ORMS maps required resampling of the original data set at equal intervals (5 km) and therefore every point could be shown on the map. The CPS Radian program doesn't require any resampling; it was possible to use the whole data set and distance between the nearest water depth recordings was sometimes as small as 300 m. Although the density of original sampling in digital records varies considerably for most of the NGDC surveys, we've shown every 20th data point on the overlay map.

The second overlay map shows sites of geological sampling, carried out not only by AGSO, but by all previous geological surveys in the area. There are three types of sites: dredge locations, core stations and free-fall gravity grab stations (Fig. 8). An index to the left of a sampling site shows an abbreviated name of the survey. Because of the small scale of the

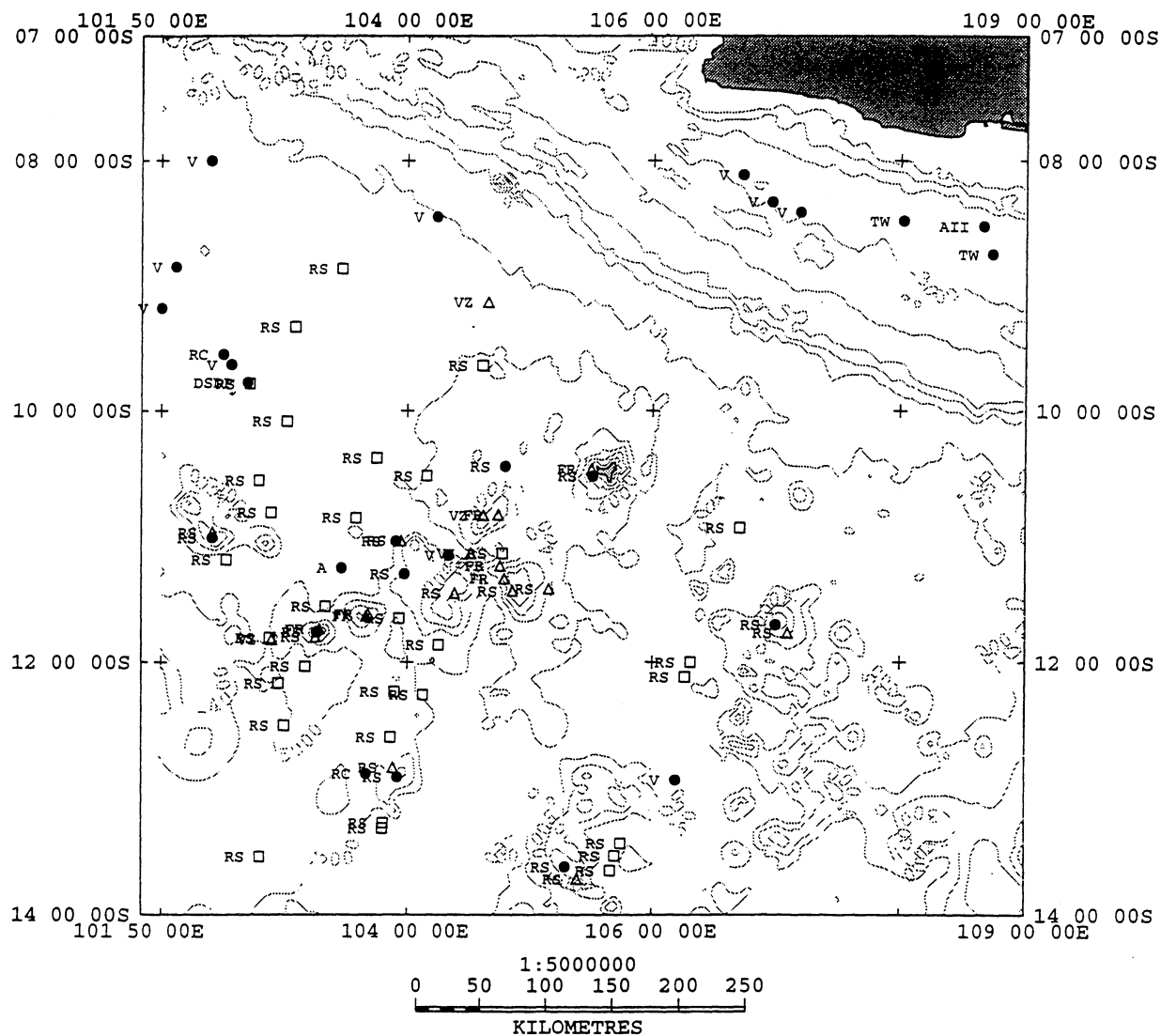


Fig. 8. Locations of geological stations in the Christmas Island area. Bathymetry is shown with a 1000 m interval.

- △ dredge sites
- gravity and piston cores
- free-fall gravity grabs

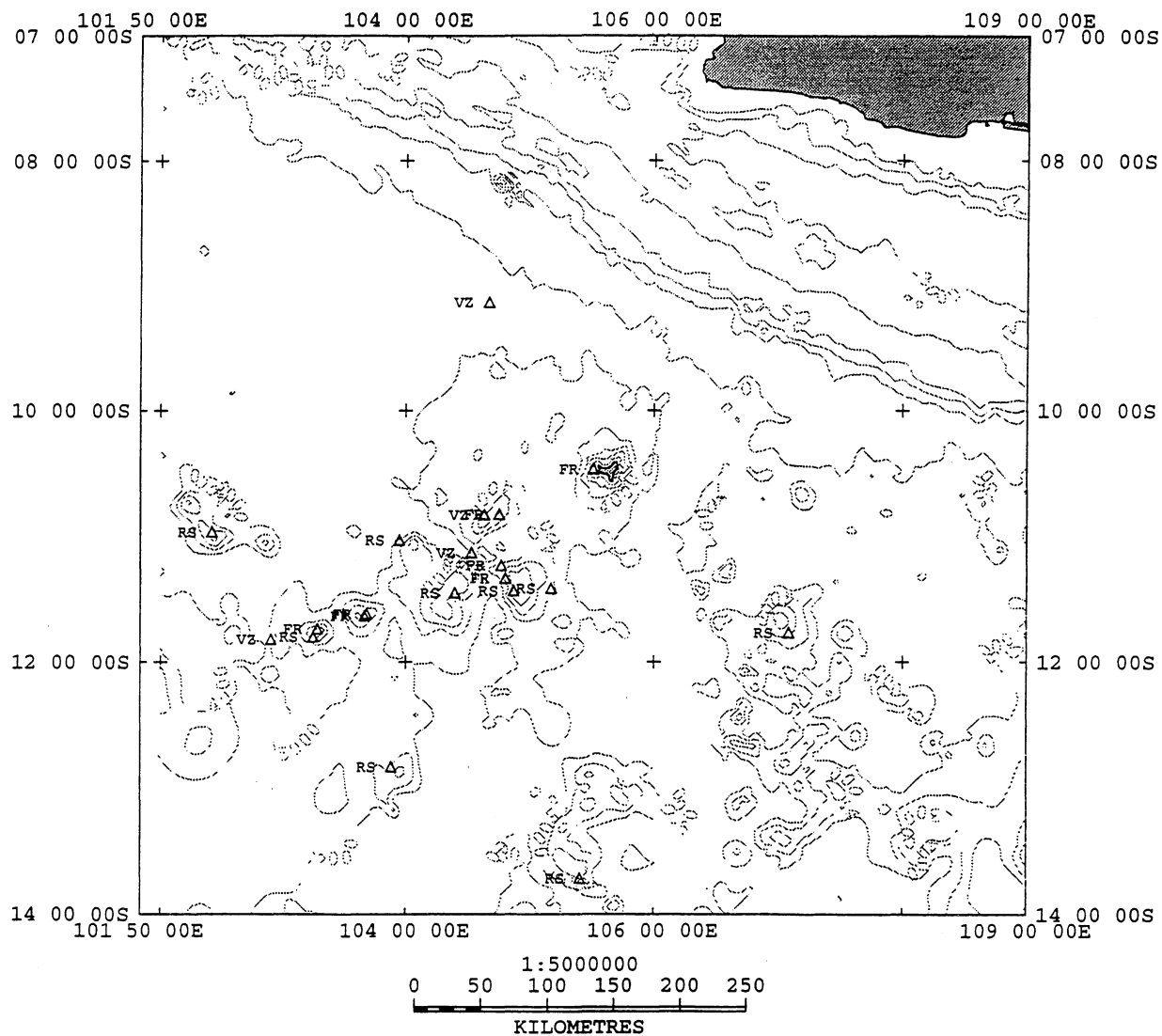


Fig. 9. Locations of the dredge sites.

RS - "Rig Seismic"; FR - "Franklin"; VZ - "Vitiaz"

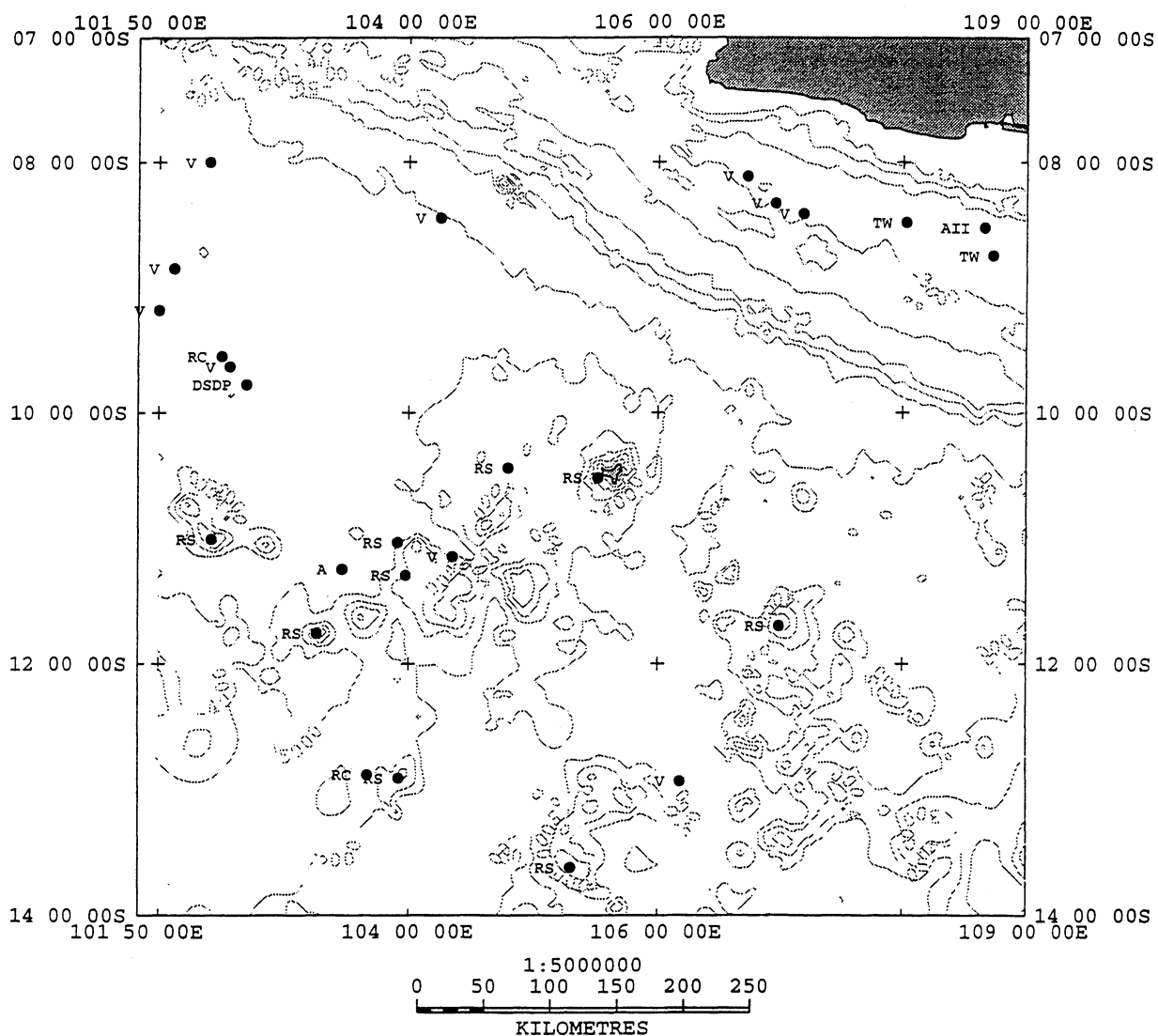


Fig. 10. Locations of core sampling.

RS - "Rig Seismic"; RC - "Robert Conrad"; A - "Argo"; V - "Vema"; AII - "Atlantis II";
 TW - "Thomas Washington"; DSDP - "Glomar Challenger"

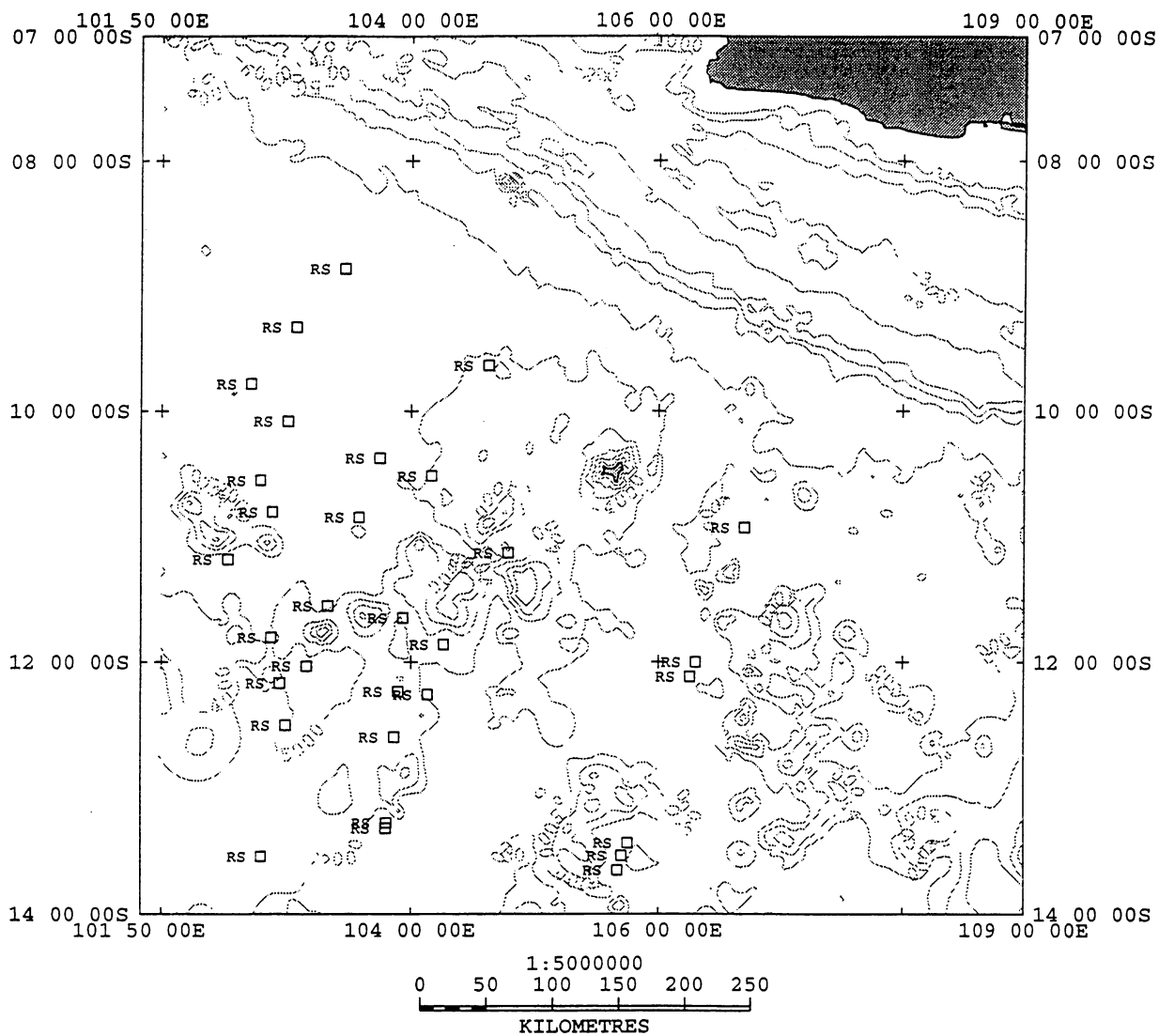


Fig.11. Locations of the free-fall gravity grab sites.
RS - "Rig Seismic".

figures, we had to show indexes on separate figures (Fig. 9-11), corresponding to each type of stations.

COMPILATION OF A SEDIMENTARY THICKNESS MAP

The Christmas Island region, being located within a deep-sea environment was never an area of interest for petroleum exploration, and therefore only a few scientific institutions carried out seismic surveys here (Fig.12). A list of surveys, the data of which were used for the sediment thickness map compilation, is presented in Table 3. Sediment thickness values were digitised from microfilms with analog records, at an hourly interval (which corresponds roughly to 15 km), and combined with navigation data. The whole data set of sediment thickness values contains 1074 points.

Table 3. Surveys with seismic reflection profiling used for compilation of the sedimentary thickness map.

COUNTRY	INSTITUTION	PLATFORM	PROJECT	PORTS (START-FINISH)	DATES (WITHIN THE CHRISTMAS ISLAND AREA)
AUSTRALIA	AGSO	RIG SEISMIC	CRUISE 107	CHRISTMAS ISLAND - CHRISTMAS ISLAND	7/1/1992-4/2/1992
USA	LAMONT-DOHERTY GEOLOGICAL	R. CONRAD	CRUISE 14	SINGAPORE-DARWIN	9/4/71-22/4/71
		VEMA	CRUISE 19	SINGAPORE - COLUMBO	16/7/63 - 18/7/63
		VEMA	CRUISE 24	DARWIN - PORT LOUIS	1/9/67 - 3/9/67
		VEMA	CRUISE 28	DARWIN - SINGAPORE	10/11/71 - 11/11/71
	WOODS HOLE OCEANOGRAPHIC INSTITUTION	ATLANTIS II	CRUISE 93	DARWIN - SINGAPORE	20/11/76 - 22/11/76
		CHAIN	LEG. 6		6/6/71 - 7/6/71
	NAVAL OCEANOGRAPHIC OFFICE	WILKES	LEG 17,20	SINGAPORE - SINGAPORE	21/4/78 - 24/4/78
		BARTLETT	LEG. F	DARWIN - DJAKARTA	3/9/71 - 14/9/71
		BARTLETT	LEG. G	DJAKARTA - DJAKARTA	20/9/71 - 13/10/71
		BARTLETT	LEG. K	DJAKARTA - DARWIN	13/12/71 - 18/12/71
	SCRIPPS INSTITUTE OF OCEANOGRAPHY	MELVILLE	ANTIPODE, LEG. 5	MANILA - PORT LOUIS	10/10/70 - 11/10/70
		T. WASHINGTON	EURYDICE, LEG. 5	SINGAPORE - SURABAYA	31/1/75 - 4/2/75
		T. WASHINGTON	RAMA, LEG. 5	AGANA - PADANG	14/9/80 - 26/9/80
		GLOMAR	DSDP,	DARWIN - COLUMBO	5/1/72 - 24/1/72
		CHALLENGER	LEG. 22		

Overall coverage of the area, as shown in Fig. 12, is quite good; only the southeastern and southwestern corners of the area don't have any data. However, with topography being

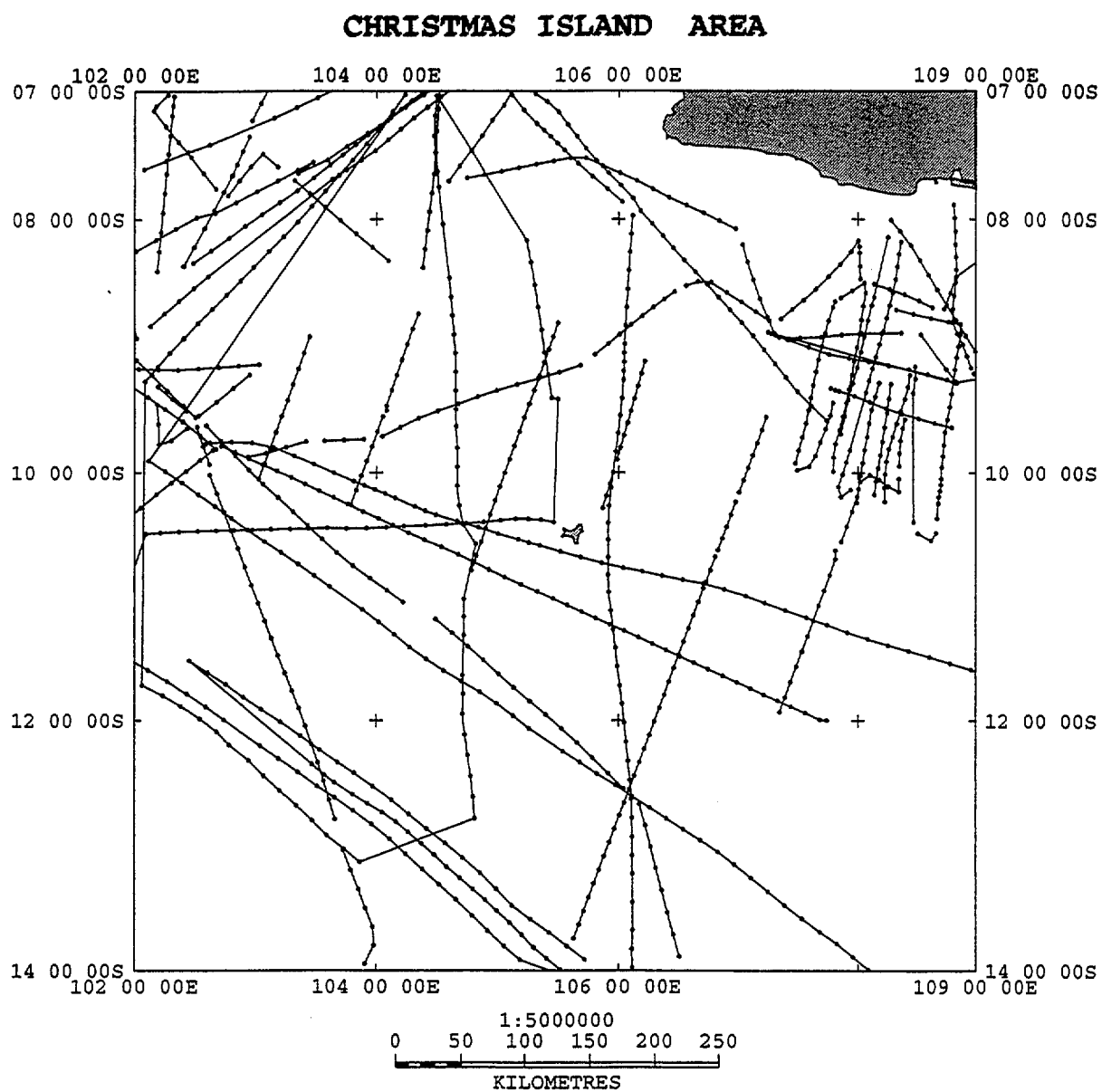


Fig. 12. Tracklines of the seismic surveys in the Christmas Island area.

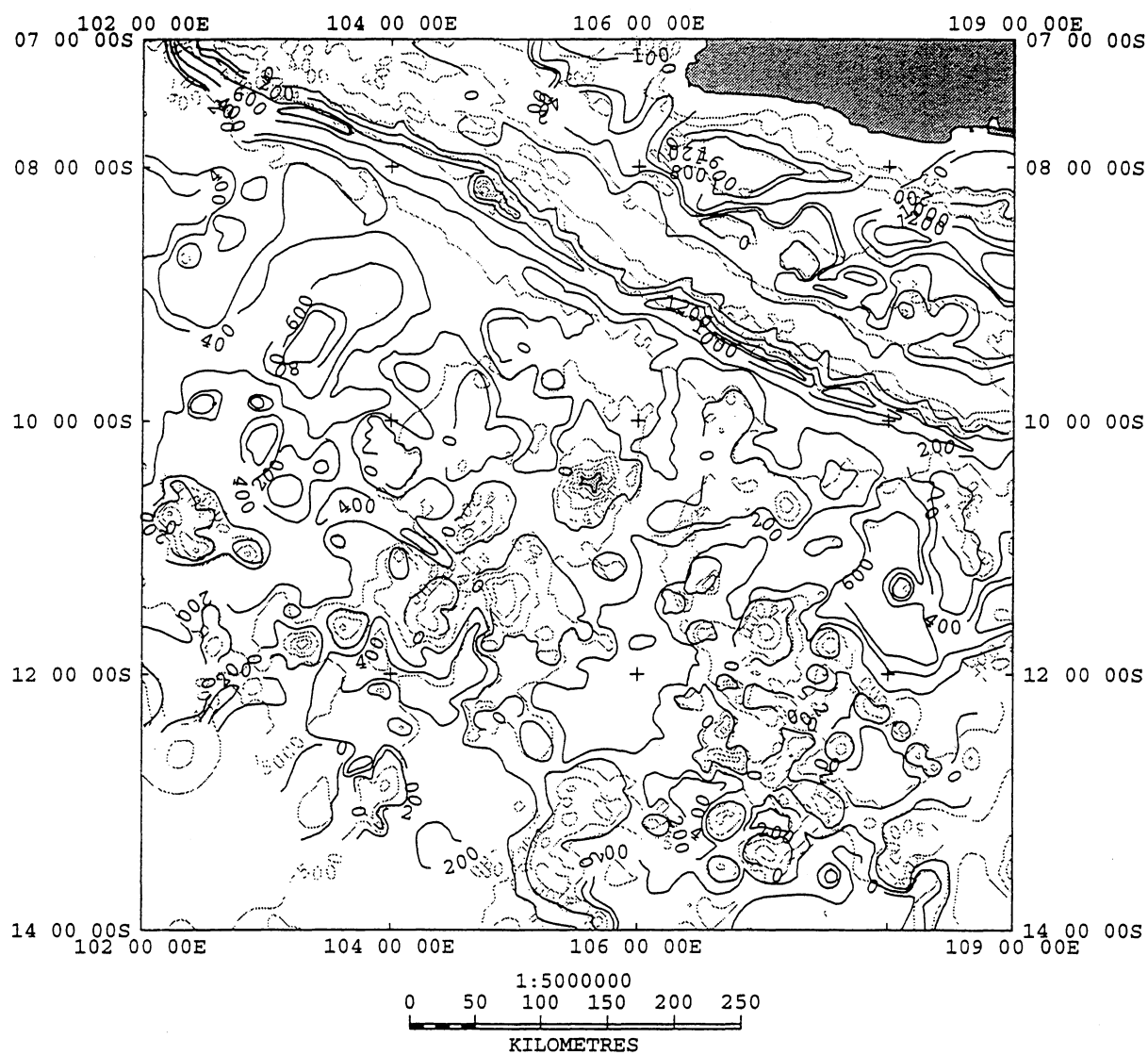


Fig.13. The sedimentary thickness map. Isopach map in 200 m contours;
1000 m bathymetric contours - faint colour .

extremely rough, a complicated pattern of seamount distribution, and the average spacing between tracks equal to 100 km, interpretation of the data becomes very difficult.

Our judgement on sediment distribution was made with strong reference to the new bathymetric map (Fig. 13). The sedimentary thickness map was originally compiled manually on a light table, overlying the new bathymetric map by a map of sediment thickness posted values. Then it was digitised, checked on the screen, and slightly edited.

SEAFLOOR MORPHOLOGY AND TECTONICS IN THE CHRISTMAS ISLAND AREA

Christmas Island is located approximately 300 km south of the Java Trench, a major tectonic boundary dividing the Indian plate from the island-arc complexes of Indonesia. A broad zone of earthquakes is associated with this subduction zone (Fig. 14). The Indian Ocean floor is sliding approximately northward beneath Java at a velocity between 7.0 and 8.0 cm/yr (Fig. 15); the convergence direction is 020° (Seno and Eguchi, 1983). The magnitude and depth of the earthquakes changes along the Sunda Arc. Numerous large earthquakes were registered near Sumatra, but there is little evidence to support the occurrence of such events near Java (Fig. 14). Seismotectonic studies (Newcomb and McCann, 1987) showed that earthquake occurrence is affected by convergence rate and direction, age of the subducted plate and dip of the Benioff zone. In comparison to Central Java, where convergence is almost frontal and subsiding lithosphere is old (Early Cretaceous), near Sumatra convergence is oblique and younger lithosphere (Late Cretaceous-Paleocene) is carried into the trench. Younger lithosphere is more buoyant, and the width of the plate interface is therefore much broader than in the case of old lithosphere. This causes large interplate earthquakes under Sumatra. The width of the plate interface under Java is much narrower and the Benioff zone dips more steeply (Newcomb and McCann, 1987), which explains relatively aseismic subduction here. Sunda Strait is the major transition zone between the two modes of subduction (Moore et al., 1980).

In terms of seafloor morphology, the area may be subdivided into two dramatically different physiographic provinces (Fig.2): 1) Wharton Basin, the north-eastern part of the Indian plate, formed during early stages of Australia-India separation and 2) the Java Trench and forearc.

1. Seafloor in the Wharton Basin is dominated by a large number of seamounts rising from the abyssal plain. The abyssal plain generally lies at depths of 5500-5700 m below sea level. The sediment thickness usually doesn't exceed 600 m, on average varying from 200 to 400 m. When covered by more than 200 m sediment,

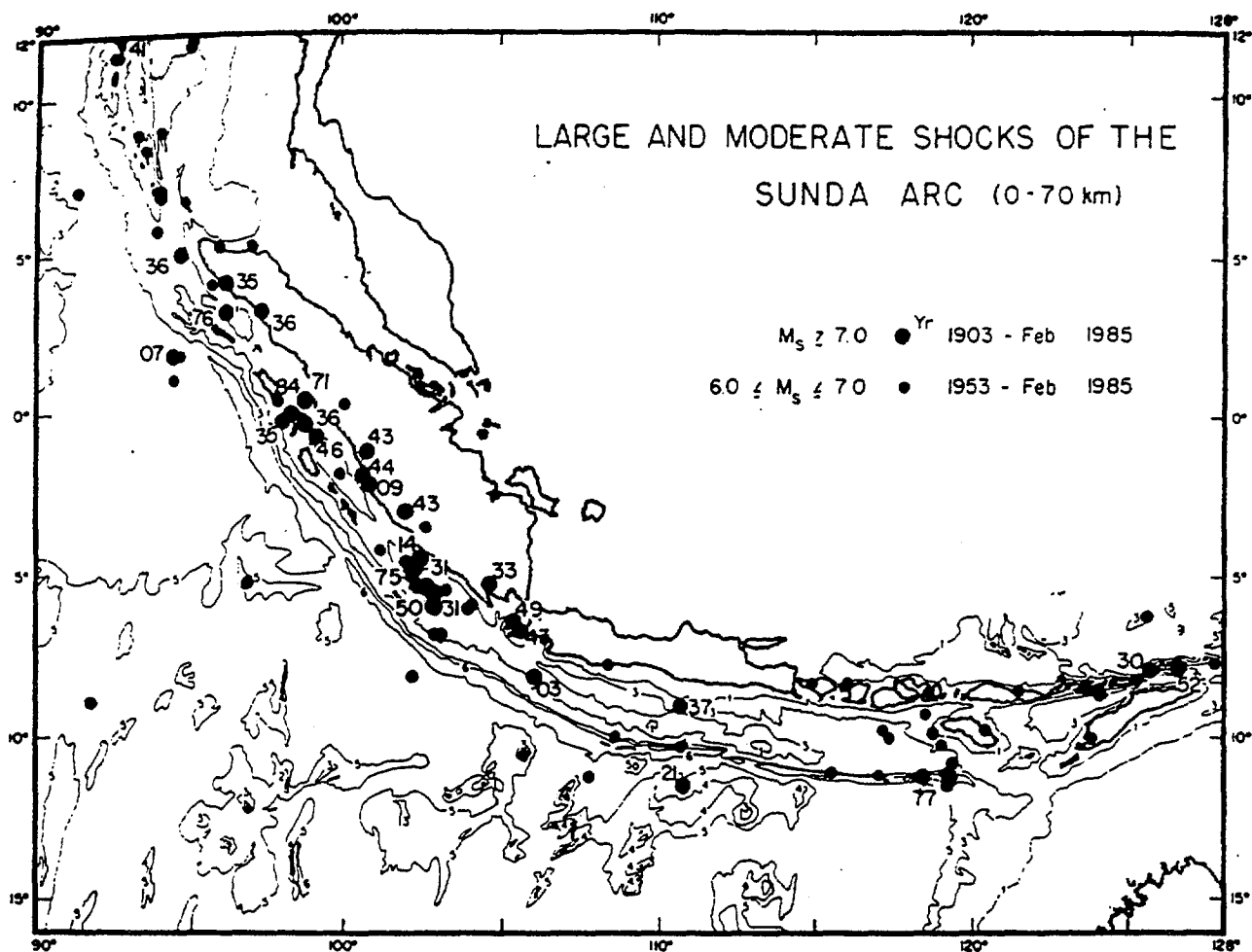


Fig. 14. Large shallow earthquakes ($M_s > 7.0$; $z < 70$ km) of this century are plotted with year beside the epicentral location (after Newcomb and McCann, 1987).

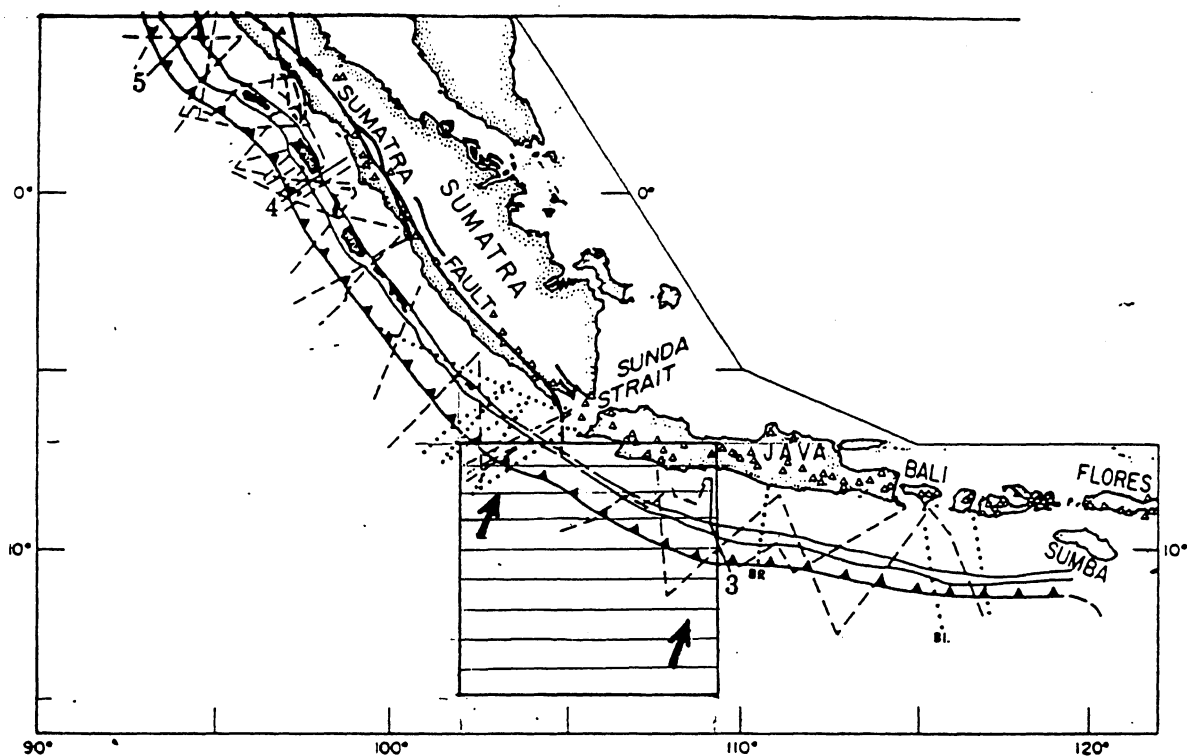




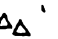



Fig. 15. Location of the study area in its geodynamic setting (modified from Moore et al., 1980).

-  directions of plate convergence
-  subduction zone
-  major strike-slip faults
-  forearc ridge
-  quaternary and active volcanoes
-  geophysical ship tracks across the trench

the seafloor is flat. Seamounts are grouped in clusters of large and small, irregularly spaced volcanoes. Seamount heights vary from 1000 m to more than 3000 m. The total height of the volcanic edifice crowned by Christmas Island is about 5000m.

2. Subduction system elements - trench, fore-arc ridge, fore-arc basins and volcanic arc - are developed here very well. The Java Trench is flanked on its landward side by the fore-arc ridge, rising generally to a depth of 2,000 - 2,500 m, with a very complicated and rough topography. Between the fore-arc ridge and Java there are fore-arc basins, underlain by thick sediments (up to 4-4.5 km, Hamilton, 1979). Within the studied area from east to west considerable changes in the trench and forearc structure are observed, consistent with changes in the mode of subduction (Fig. 16).

The Java trench

The floor of the Indian Ocean deflects gently downward at the outer edge of the Java Trench and typically descends only about 1,000 m across the 70-100 km width of the trench. The depth of the trench gradually increases from NW to SE, from 6,400 m off western to 7,000 m off eastern Java. The changing depth of the trench correlates in part with the thickness of sediment on the ocean floor and in the trench (Hamilton, 1979): as the overlying sediment thickens the trench floor shallows. This relationship can be clearly seen throughout all the Java-Sumatra trench system. The trench is shallowest off northern Sumatra, where the seafloor is covered by thick sediments of the Bengal fan, and off northwestern Australia and is deepest off central Java, where only thin pelagic sediments are deposited in the trench. Within the Christmas Island area, changes in sediment thickness are not very great: from 400-500 m in the western part of the region to 100 m in the eastern part. The corresponding increase in the depth of the trench to the east is of the same order. In Fig. 16, two seismic reflection profiles across the trench are presented, showing the difference in trench and fore-arc structure between eastern (a) and western (b) parts of the area.

It's very difficult to estimate accurately total sediment thickness in the deepest parts of the trench with conventional seismic profiling techniques, so our map (Fig. 13) shows only sediment thicknesses that were possible to interpret. However, real values may be considerably greater. Within the trench the terrigenous sediments cover the abyssal sediments. Most of the terrigenous sediment from Java are trapped closer to the island, in the fore-arc basin. If they reach the trench they are quickly added to the melange wedge by tectonic accretion (Hamilton, 1979).

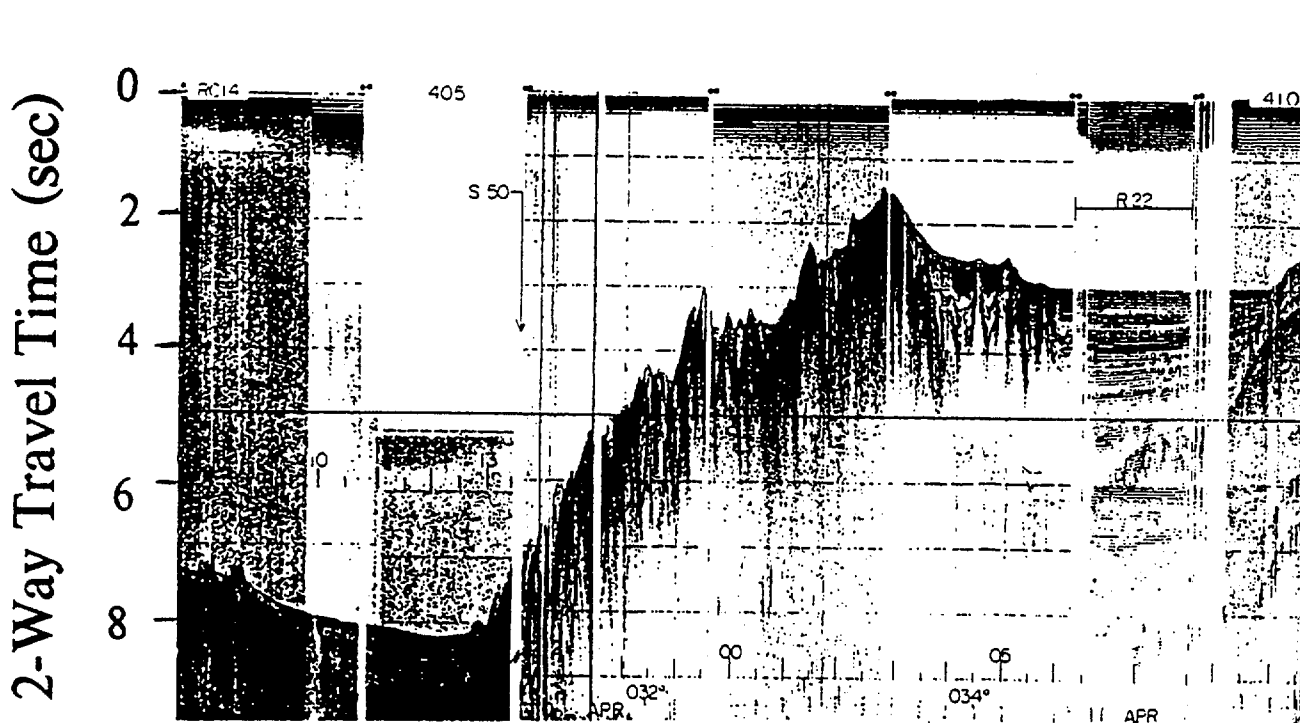
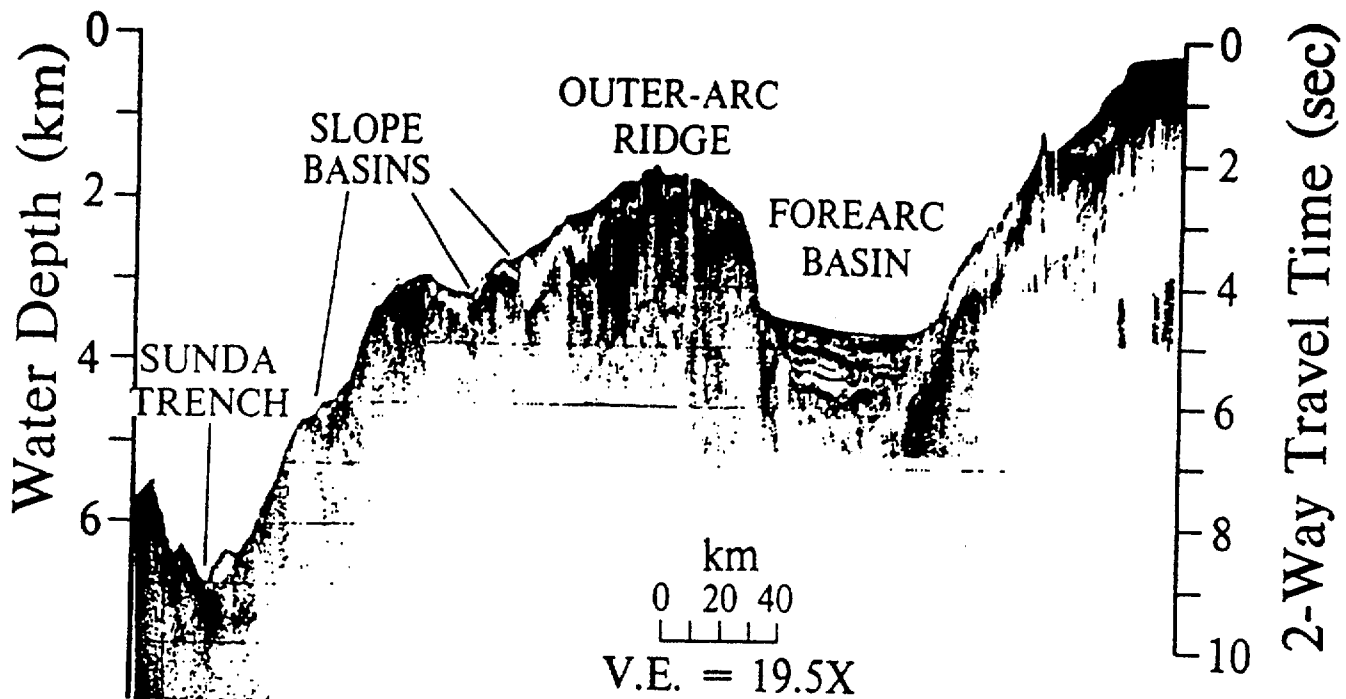


Fig. 16. Single-channel analog seismic reflection profiles across the Sunda Trench
a) in the Java province at about 110° E (Scripps Oceanographic Institute, Eurydice expedition); b) in the South Sumatra province at about 103° E (Lamont-Doherty Geological Observatory, Conrad 14)

Apart from the general trends described in the previous works (Curry et al., 1977; Hamilton, 1979; Moore et al., 1980), our bathymetric and sediment thickness maps display a number of new interesting features in trench morphology. The trench can be subdivided into a few individual segments separated by transition zones. Each segment has maximum width and depth in the middle of the segment, and narrows and shallows to the edges. The lengths of the segments vary from 70 to more than 100 km. The transition zones commonly lie close to seamounts or ridges approaching the trench, or on the continuation of the Indian plate fracture zones. There is no visible displacement between the segments. Transition zones represent shallow "saddles" between deeper parts of the trench, and sometimes mark a deviation from the general trend of the trench.

Similar elongate local deeps within the Java Trench, divided by zones of irregular topography, were described to the east of the studied area, between 108° and 120°E (Masson et al., 1990). Here GLORIA (long-range side-scan sonar) images have demonstrated that local deeps in the trench axis are, at least in part, a consequence of seamount collision, since the retreat of the deformation front which results from collision exposes deeper levels of the subducting plate.

A major deviation in the trench's strike occurs between longitudes 105°30' and 106°E, where the Christmas Island Rise approaches the trench. Christmas Island itself is almost 300 km from the trench, but it resides on an elevated block, or rise, which in the vicinity of the trench is at least 600 m higher than adjacent parts of the seafloor. Within this area the trench narrows considerably (to about 40 km across) and, although the depths here are the same as in other parts of the trench, it represents a shallow segment in the basement structure. This is because sediment thickness here is only about 400 m, whereas in the adjacent segments it exceeds 1000m. The difference in basement elevation reaches 600-800 m, which is comparable with the elevation of the Christmas Island Rise itself.

Masson (1990) describes a similar impact of the Roo Rise on the trench structure between 112° and 115°E, where the trench floor becomes anomalously shallow. The Roo Rise continues into the trench, as is shown by the axis of the trench being deflected 50-60 km landward, and the great thickness of the crust (Newcomb and McCann, 1987). Masson also described a recent uplift of the trench-slope break in an isolated region immediately landward of the Roo Rise. Based on these observations Newcomb and McCann (1987) suggested that substantial parts of the rise's northern flank have entered the trench. The low-density root of the Roo Rise should cause this bathymetric feature to be more buoyant than the surrounding seafloor, and therefore more difficult to subduct. Obviously the changes in the trench and forearc ridge structure near the Christmas Island Rise are not so

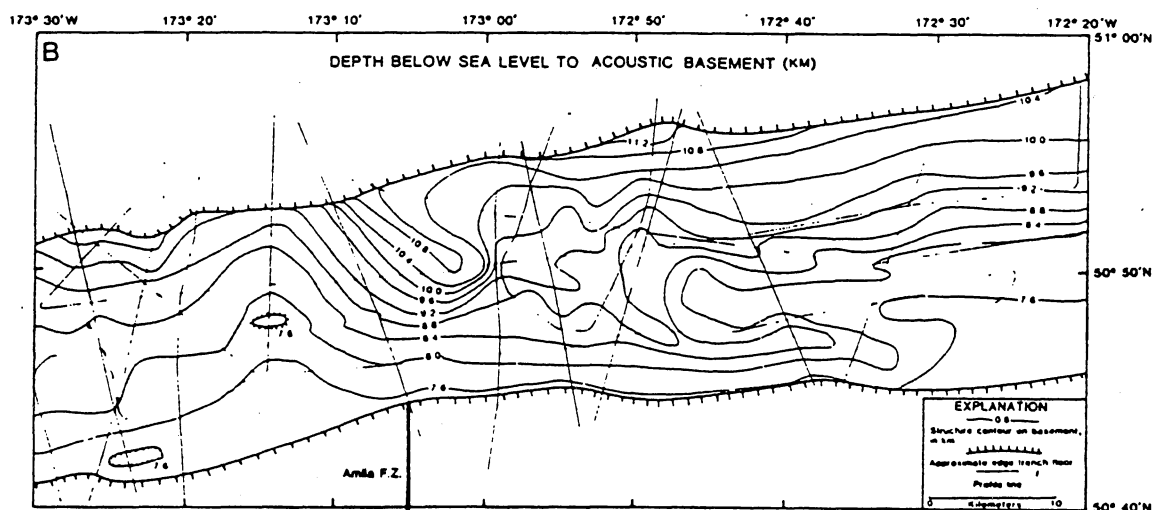
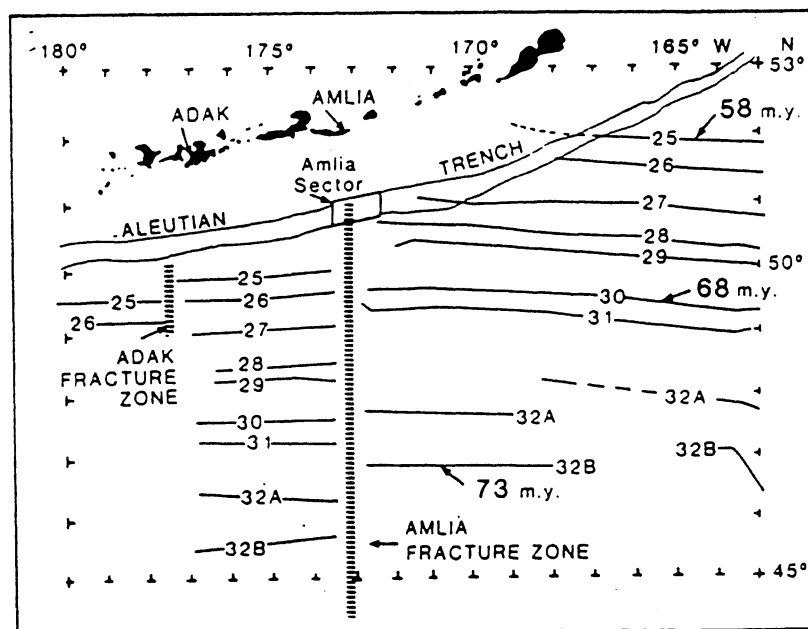


Fig. 17. Example from Aleutian Trench (from Scholl et al., 1982) illustrating changes in the basement structure at the intersection with a large former transform fault: a) magnetic lineations displaced by the Amlia fracture zone; b) contours of the trench basement in km.

profound as in the case of the Roo Rise, but shallowing of the trench suggests that we may be observing an early stage of rise-trench interaction.

To the west of the Christmas Island Rise, the trench is generally wider, and the slope break on its seaward side is not always well defined. The trench floor is either flat or gently dipping towards the trench axis. Sediment thicknesses vary from 400 to more than 1200 m, maximum thicknesses being found close to the steep slope of the fore-arc ridge. This part of the Java Trench can be subdivided into 3 segments: 101°30' - 103°E; 103° - 103°50' and 104° - 105°30'. The westernmost of them is the shallowest (average depth 6200 m) and relatively narrow. In the second, depths increase up to 6600 m and sediment thickness exceeds 1000m. The boundaries of these two segments appear to be on the continuation of N-S trending lineaments, which are most likely to be old transform faults of the Late Cretaceous - Palaeogene spreading system.

The impact of seafloor spreading fracture zones on trench structure has been studied by Scholl et al. (1982), using the example of the Amlia Fracture zone subsiding into the Aleutian Trench. According to their seismic data there is an abrupt change in basement depth on the continuation of the Amlia FZ (Fig. 17). Within the trench floor the basement deepens to the east of the fracture zone where, according to magnetics, the subsiding crust is about 10 my older than to the west. The most abrupt change in the basement depth is adjacent to the trench inner wall, and towards the seaward boundary of the trench the differences gradually disappear. Basement irregularities are expressed in trench bathymetry as a series of deeps separated by shallower areas. Data presented by Scholl et al. (1982) suggests reactivation of old fracture zones and normal faults associated with seafloor spreading in the process of subduction. Our data (seismic reflection profiles) is too sparse to identify such structures, but we suggest that some boundaries (or transition zones) between the segments are related to reactivation of fracture zones on the subducting plate (Fig 18-tectonic map).

The third segment has a complicated structure: one large and at least 2 smaller seamounts are rising from the bottom of the trench. They are bounded by a series of isolated depressions more than 7000 m deep. The steep slope of the fore-arc ridge behind the seamounts displays a clear deviation of its strike landwards, creating a large crescentic feature.

A number of authors have demonstrated the effect of seamounts being carried into a trench and colliding with a forearc (Fryer and Smooth, 1985; Lonsdale, 1986; Kobayashi et al., 1987; Masson et al., 1990). It has been shown that collision with the forearc can result in varying degrees of deformation of the forearc region (Fig. 19). Landward re-entrants in

TECTONIC INTERPRETATION

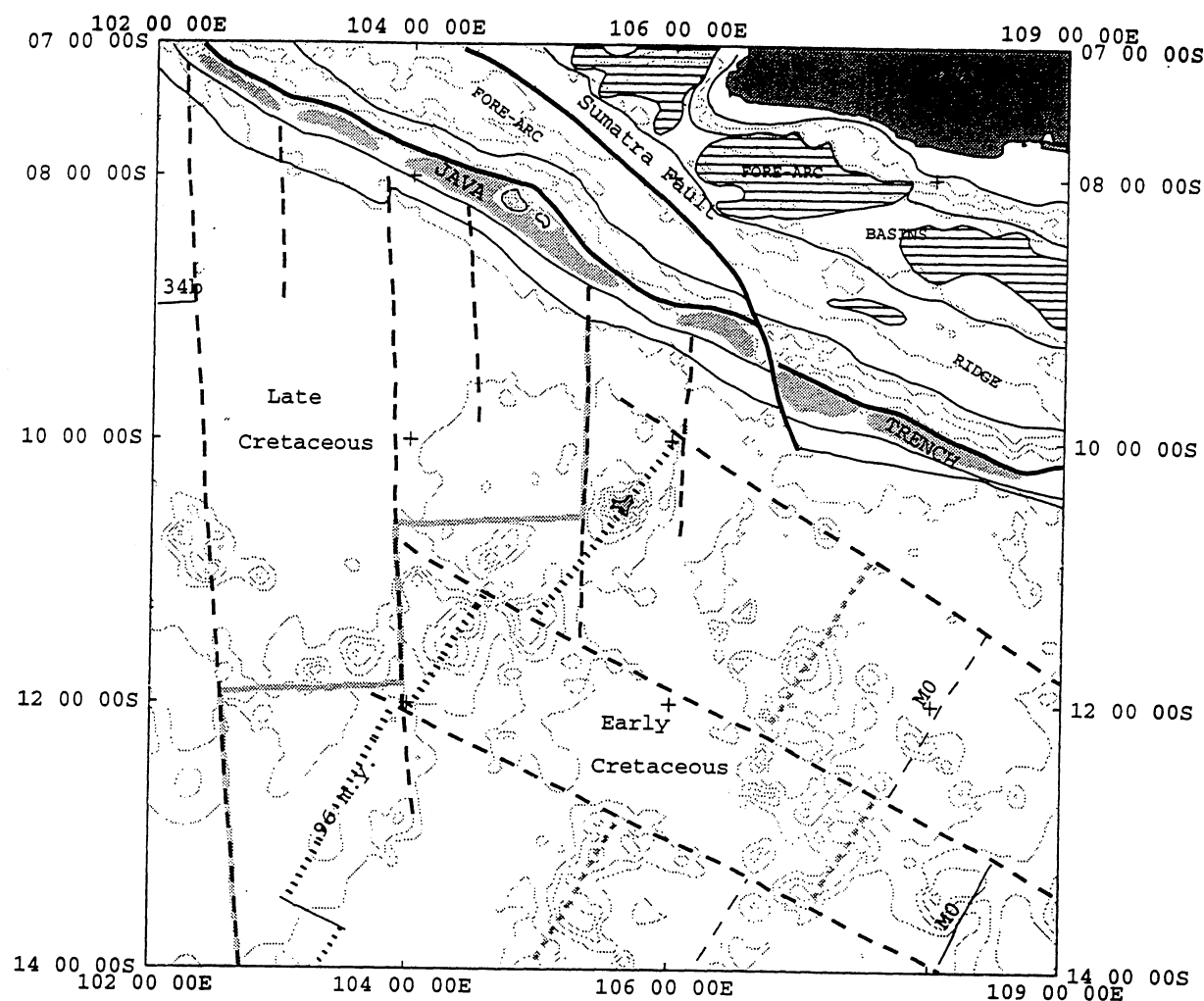
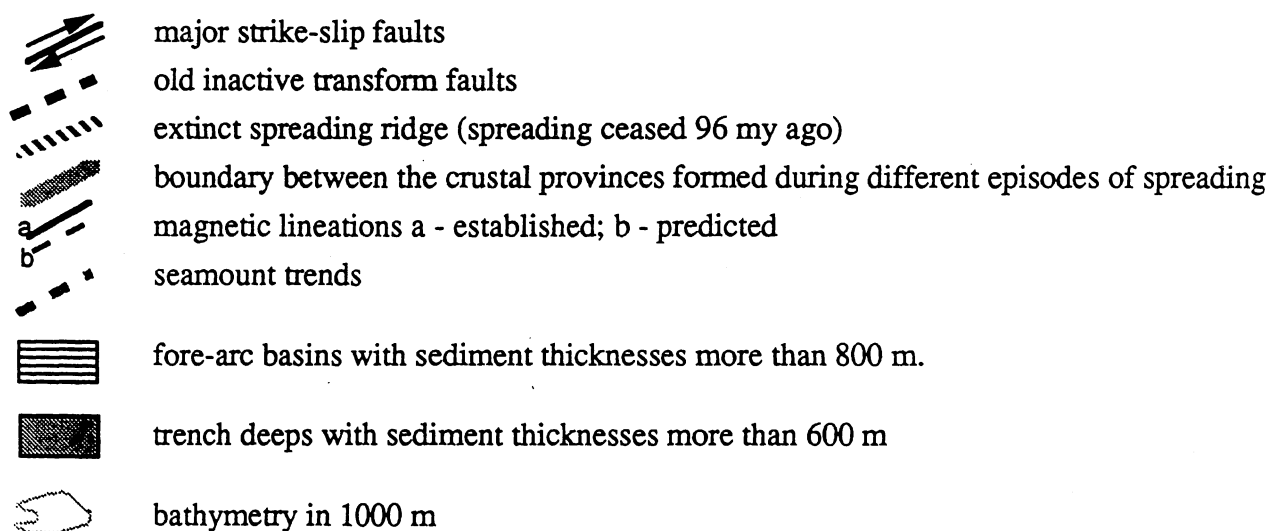


Fig. 18. Tectonic map of the Christmas Island area.



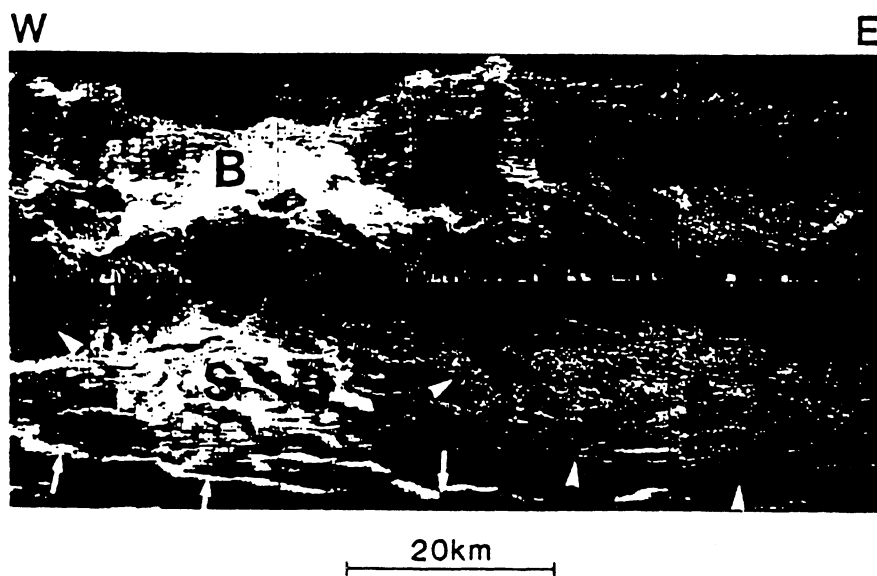
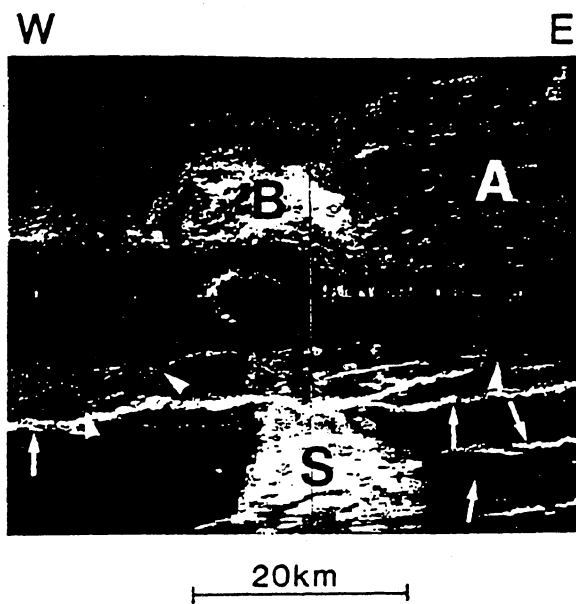
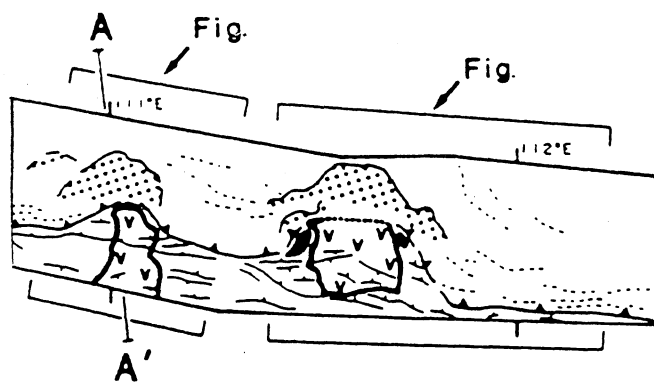


Fig. 19. Interpretation of Gloria images (a) and original sonographs showing seamounts at different stages of collision with accretionary wedge (b) early stage; (c) advanced stage (after Masson, 1990).

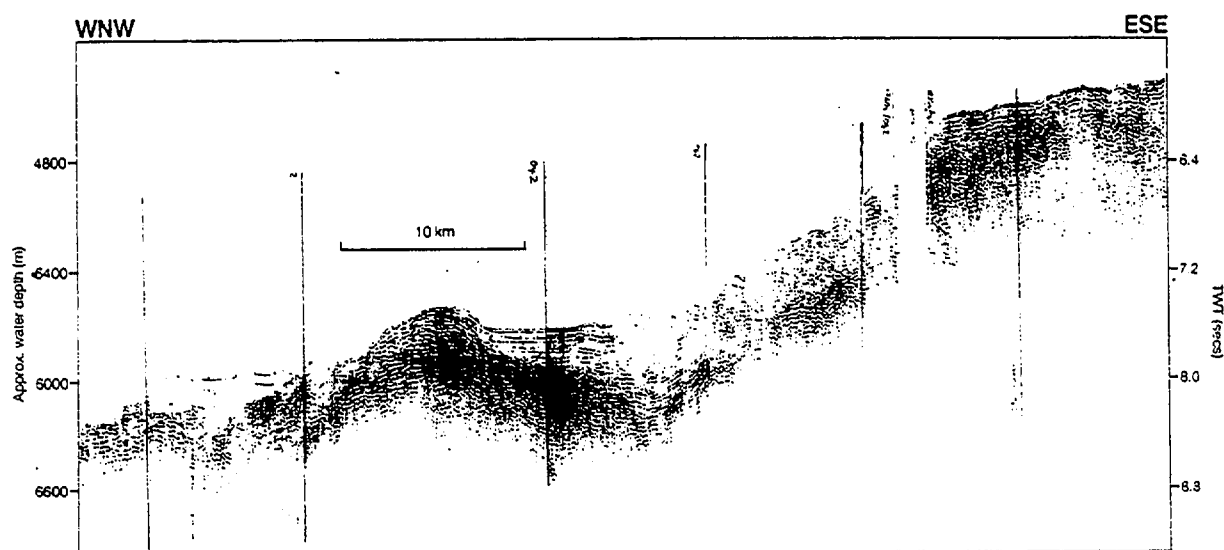
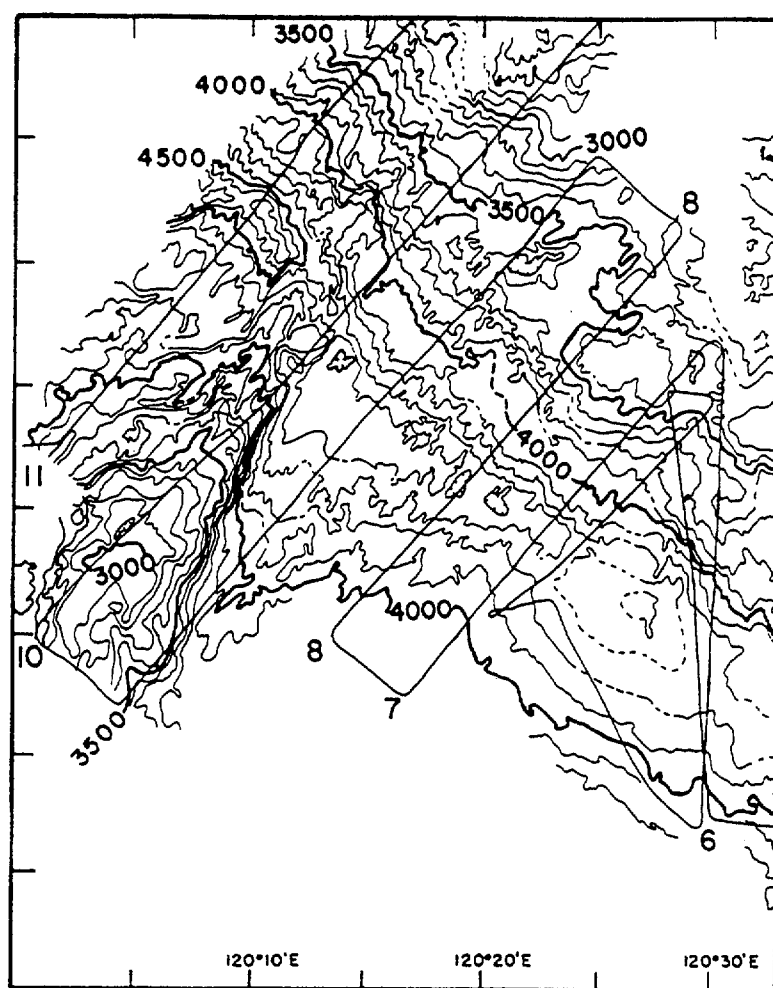


Fig. 20. A. SeaMARC II bathymetry of the eastern termination of the Java Trench; a seamount colliding with the accretionary wedge (after Breen et al., 1986). B. Single-channel seismic section across the northern edge of the seamount shown above (after Milsom et al., 1992).

the deformation front (Fig. 20), where seamounts collided with the accretionary wedge, have been observed in the Eastern Java Trench (Breen et al., 1986; Masson et al., 1990; Milsom, 1992), south of the island of Sumba (Breen et al., 1986), and in the Japan Trench, where they have been related to completely subducted seamounts (Lallemand and Le Pichon, 1987). We suggest that the crescentic steep slope at about 105°E behind the seamounts on the bottom of the trench, originates from their collision with the forearc.

To the east of the Christmas Island Rise the trench deepens, and sediments concentrate in a narrow strip along the steep slope of the forearc ridge, their thickness at places exceeding 1200 m. Within this part of the trench we identified one long segment, between 106°50' and 108°40', and two short segments to the west and to the east. A transition zone at 106°50' lies on the continuation of the major strike-slip fault of the region, the Sumatra Fault System. This system extends for 1600 km along the volcanic arc of western Sumatra and may be traced into the fore-arc south of Sumatra as a complex series of extensional faults (Huchon and Le Pichon, 1984). Within the studied area, the fault zone was identified between 104°E 6°S and 106° 50'E 9°S on the basis of bathymetric data (Fig.18). There is a sudden increase (almost doubling) in width of the trench to the east of the transition zone. Here the trench reaches its maximum width (about 100 km) and then gradually narrows (to less than 50 km) towards the next transition zone. The development of this area can be understood by considering the entire Sumatra margin as a discrete tectonic block (Curry et al., 1978), defined by the right-lateral Sumatra Fault System.

Newcomb & McCann interpreted the landward deflection of structures in the fore arc to be along the trailing edge of a block of forearc basement, which is being displaced northwest with respect to the Sundaland platform of Sumatra and western Java. This model predicts extension within the trailing edge of the upper plate. Extensional structures in Sunda Strait (Fig. 21) were identified on the seismic reflection profiles recorded in 1985 during the French-Indonesian cruise "Krakatau" (Lassal et al., 1989). It was suggested that they are related to the Sumatra Fault Zone and explain the opening of the strait since the last 5 Ma. The subducted plate here appears to have a more shallow dip, as inferred from the gravity signature. Therefore the sudden widening of the trench may be interpreted as a result of less horizontal compression of the oceanic plate prior to subduction in the region, where the upper plate is displaced.

To the west of 108°40', the trench structure is very disrupted; it consists of short segments or depressions, covered with a very thin layer (about 100 m) of sediments. Disruptions in the internal structure of the trench are caused here by a series of seamounts carried into the trench.

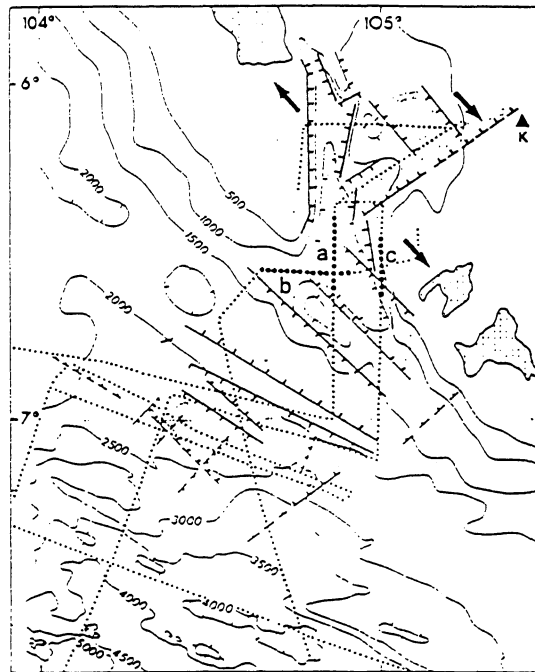


Fig. 21. Extensional structures in Sunda strait on the continuation of Sumatra fault system (after Lassal et al., 1989)

The forearc ridge

The continental slope rising from the Java Trench is formed of sediments deformed complexly by subduction and gravitational processes. The slope rises steadily but irregularly to the outer-arc ridge, whose crest lies half way between the trench and Java. The fore-arc ridge consists of two large arcs, joining together near the westernmost point of Java. The eastern arc, Java Ridge, bounds the Sunda Trough and the western arc, extending to the north (Mentawai Ridge), separates Mentawai Basin from the Sunda Trench. Both the Sunda Trough and the Mentawai Basin are forearc basins filled with thick sediments.

The forearc ridge in the area is a wholly submarine feature and its crest lies at about 2000 m below sea level. The continental slope and the ridge crest are underlain by a wedge of melange and imbricated sediments (Hamilton, 1979). The height of the ridge is greater off Sumatra than off Java. The scraping off of terrigenous sediment is considered to be the major factor in the growth of the wedge. Because the volume of these sediments is very little off Java and it increases towards Sumatra, it was suggested that the height of the forearc ridge depends upon the thickness of terrigenous sediments on the subducting plate.

The seaward slope of the Java Ridge consists of two distinctive parts: very steep and rough slope hardly covered by any sediments rises from the bottom of the trench to about 3500 m and the upper part of the slope gradually rises to the crest (2000 m) of the ridge (Fig.16). The upper part of the slope consists of a series of steps divided by outcrops of basement and covered by up to 300 m of sediment. The crest of the ridge lies very close to the forearc basin. The slope facing the basin is steeper than the outer upper slope described above, and has a simple uniform structure.

The impact of seamounts colliding with the trench was discussed above. Within the studied area we observed only one example of such collision at about 105°E, resulting in the formation of a very steep crescentic slope in the lower part of the forearc ridge. According to Masson (1990) this impact on the forearc structure reflects the early stage of seamount collision. Later stages may be expressed in bottom topography as distinctive highs on the fore-arc ridge. Often these highs occur landward of some major indentations in the accretionary wedge, particularly where seamounts have been subducted completely (e.g. at 109°E, between 109°45' and 110°45'). Less obvious, but still recognisable high on the forearc ridge slope occurs landward of the crescentic feature described above. This effect was predicted by the model of Lallemand and Le Pichon (1987), which indicates that

subducted seamounts will continue to cause uplift of the forearc as the subducting plate carries them several ten of kilometres landward of their site of subduction

Fore-arc basins

Most sediment from Java is deposited in the fore-arc basins, the forearc ridge barring it from the trench. The floor of the basins is usually smooth, water depths being typically 3,400-3,600 m. Thick sediments lie beneath most of the basins and their thickness in places reaching 4.5 km (Hamilton, 1974). The basin sediments are deformed, gently near and then more severely toward the forearc ridge. Deeper reflections are missing near the ridge and it was suggested (Hamilton, 1979) that the ridge was formed largely of deformed sediments equivalent to those in the basin.

Our sediment thickness map (Fig. 13) shows that the Sunda Trough, that was shown on the previous maps as a single fore-arc basin (Map of sedimentary basins of the Indonesian Region; 1974; Tectonic map of the Circum-Pacific Region, 1991), consists of several en-echelon depressions in the basement masked by the sediment fill. Sediment thickness in these depressions often exceeds 2000 m, sometimes reaching about 4000 m, whereas basement highs, separating the depressions, are covered only by up to 800 m of sediment. The depressions have an elongated shape with their axis being oriented slightly oblique to the trench; they have almost latitudinal orientation. The typical size of the depressions is about 70-80 km long and 30 km wide.

Oblique trends in fore-arcs have been recognised in different subduction systems: Kuril (DeMets, 1992), Sumatra (McCaffrey, 1992) and Aleutian (Geist et al., 1988). The origin of the oblique forearc basins in the Aleutian Arc was explained by block rotation, caused mostly by oblique convergence (Geist et al., 1988). Another example of fore-arc basin segmentation is off central and southern Sumatra, where it is divided into several sub-basins separated from each other by transverse highs (Moore et al., 1980). Convergence along the Java Province is nearly perpendicular to the trend of the trench axis, so there should be other reasons for fore-arc basin segmentation. Possibly it could reflect heterogeneity of the accretionary wedge.

The Northeastern Wharton Basin in the Christmas Island region.

The seafloor morphology of the northeastern Wharton Basin is very diverse. There are areas of almost flat plains and areas of abyssal hill topography, ridges and isolated seamounts. Flat areas of the abyssal plain are mostly confined to the northwestern part of the region, to the north of 10°S and to the west of 104°E. Here the seafloor lies at about 5400 m, being slightly deeper (5500-5600 m) between 103° and 104°E. Sediment thickness in this area

varies from 200 to 1000 m. Over most of the plain, sediment thickness is about 400 m and only within a linear basement depression trending NE-SW between 9° and 10°S does it rapidly increase up to 1000 m. Another relatively flat area lies about 108°E, with water depths gradually increasing towards the trench from 5400 to 6000 m. Maximum sediment thickness registered here is about 800 m at 11°40'S.

Between the flat areas and major seamount province there are areas characterised by small-scale roughness, varying sediment thickness (0-200 m), and frequent outcrops of the basement. Abyssal hill heights vary from 30-40 m to 200 m. In areas of basement ridges and larger seamounts the sediments are found only in small pockets between the peaks and in narrow gulfs between the seamounts.

Large seamounts rise up to 3000 m from the seafloor. Smaller peaks accompanying larger seamounts are commonly about 1000 m high. Morphology of the seamounts clearly indicates their volcanic origin. Most of them have very steep slopes and almost circular conical shapes. The seamounts are grouped in clusters of large and small volcanoes. All seamounts can be divided into 2 groups:

1. Seamounts located on the continuation of the Vening-Meinesz seamounts. Trending NE-SW within the region they represent a chain of densely spaced large seamounts, one of which rises above sea level - Christmas Island. Seamount summits are frequently above 2000 m below sea level, usually being 40-50 km in diameter. Geological sampling of the seamounts showed that they represent ancient volcanoes of Late Cretaceous age. These volcanoes are superimposed on a large uplifted block, 800-1000 m above the rest of the abyssal plain. The edges of this "plateau" are clearly seen on the seismic profiles. A great number of smaller seamounts (about 1000 m high) are confined within this boundary. The distribution of the seamounts, and steep slopes within the plateau, display lineations of two directions: N-S and NW-SE. They are expressed in bottom topography in the form of steep slopes or deep gulfs intruding into the plateau. The trends of the seamounts (NE-SW) seem to be displaced along NW-SE fracture zones.

2. Seamounts located in the eastern part of the area. The general trend of these seamounts, NE-SW, is similar to that of the previous group, but they are not associated with any uplifted area. Seamounts here are smaller in size, their summits usually lie at about 3000 m, and they are 20-30 km in diameter (except for the northernmost seamount - Cygnet Seamount). NW-SE lineations can be clearly traced on the continuation of lineations intersecting seamounts of the

previous group, however the other set of lineations (N-S) is absent here. The seamount chain seems to be displaced along the two most prominent NW-SE lineations (Fig. 18). Samples of volcanic rocks recovered in this area have the same range of ages as the previous group, mostly Late Cretaceous (up to Maastrichtian).

These observations allow us to suggest that both groups of seamounts were formed before or during the period when NW-SE fracture zones were active. However, the western group of seamounts may have undergone the second stage of tectonic activity, either involving uplift of the area, or extensive volcanism, associated with the new N-S trending fracture zones.

Crustal age in the northeastern part of the Wharton Basin is controversial. The eastern part of the area, adjacent to the Roo Rise, was formed during an episode of spreading following the breakup of India and Australia at 132-118 Ma (Fig.22). The westernmost part of the region was formed much later, in the Late Cretaceous (about 80-70 Ma). No identifiable magnetic anomalies were found within the major part of the area (Tectonic map of the Circum-Pacific Region, southwest quadrant, 1991; Powell et al., 1988). Plate tectonic reconstructions of the Indian ocean (Audley-Charles et al., 1988; Fullerton et al., 1989; Veevers and Li, 1991) don't give a clear picture of how and when the Early Cretaceous spreading system was reorganised to enable quick movement of India to the north. Therefore it is still very difficult to constrain the age of the crust in the vicinity of Christmas Island.

Plate tectonics of the Christmas Island area

According to the plate tectonic reconstructions of Scotese et al. (1988), a wide Tethys ocean separated India from southern Asia during the Early Cretaceous. During the Late Cretaceous, Tethys narrowed as India rifted away from Madagascar and moved rapidly northward. Rifting between India and Australia during the Early Cretaceous resulted in the formation of a new triple junction between the Indian, Australian and Neo-Tethyan plates (Fig. 23). The breakup of Australia and India occurred at 134 Ma (M10) and spreading continued at least until 118 Ma (M0).

During the Middle Cretaceous, the Tethyan rift continued to move northward as the Neo-Tethyan plate was subducted beneath Eurasia. About 95 my ago a major plate reorganisation took place. Scotese et al. (1988) suggest that this resulted from the subduction of the western part of the Tethyan Rift and elimination of the western section of the Neo-Tethyan plate. Thereafter, the Indian plate began to be subducted beneath Eurasia,

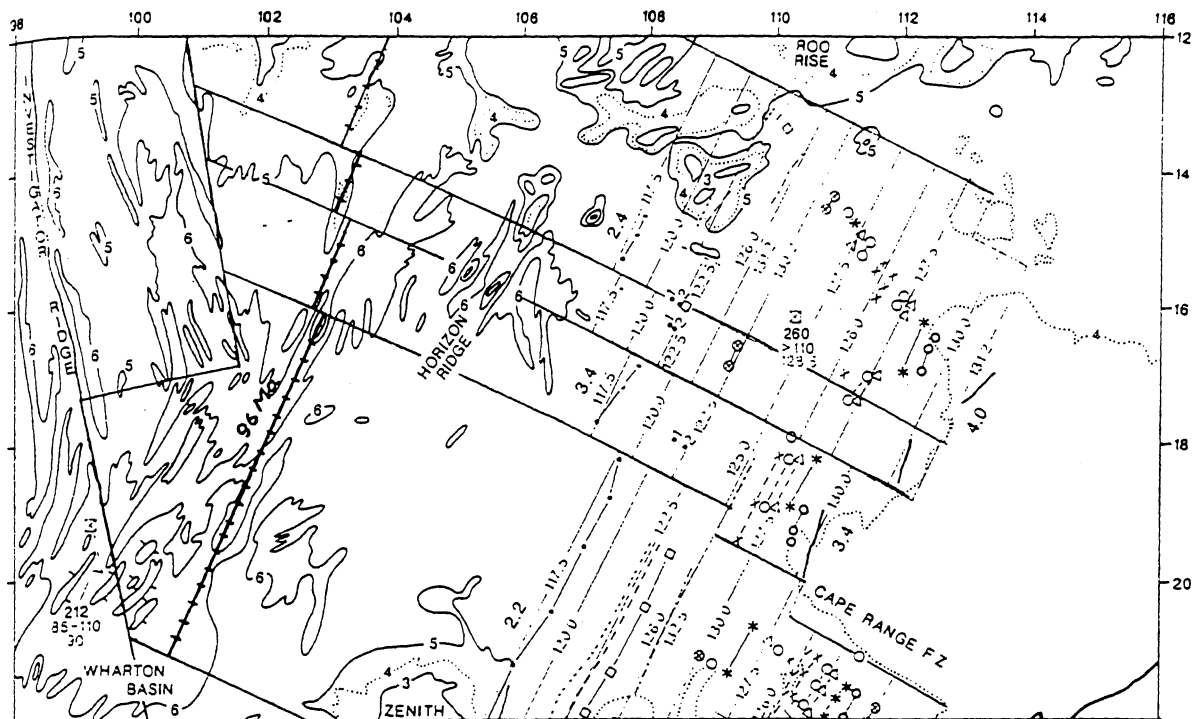


Fig. 22. Observed and inferred seafloor spreading isochrons. Predicted position of the extinct spreading axis abandoned 96 Ma ago (after Powell et al., 1988).

and this probably caused the breakup of India and Madagascar and the increase in spreading rates along the Central and Southeast Indian ridges. This plate reorganisation may also have been responsible for the drastic changes in spreading directions observed in the Wharton and Cuvier basins. In this region during formation of the Cretaceous Quiet Zone, spreading directions changed by approximately 45° , from NW to N-S (Fig. 22).

During the Late Cretaceous and Early Tertiary, India moved rapidly northward as the Indian plate continued to be directly subducted beneath the southern margin of Eurasia. In the Early Eocene, Greater India collided with Eurasia (about 50 my; Patriat and Achache, 1984). At about the time of the collision (46.2 m.y.), and possibly as a direct result of it, spreading in the Wharton Basin stopped (Liu et al., 1983), and the Indian and Australian plates were fused to form the modern Indo-Australian plate.

Early Cretaceous magnetic anomalies have been identified in the Gascoyne and Cuvier abyssal plains (e.g. Fullerton et al., 1989). They display NE-SW orientation, i.e. normal to the fracture zones described in the Christmas Island area. M0 anomaly (117.5 m.y.) lies in the southeastern corner of the area (Fig. 22). A large fracture zone, displacing this set of lineations (Fullerton et al., 1989), was extrapolated to the west where it coincides with NW bathymetric trends as far as the northern edge of the Christmas Island plateau. I suggest that the two bathymetric lineations parallel to this fracture zone, described above as fracture zones transecting seamount chains, represent old transform faults of the same generation (Fig. 18).

It has been accepted (Fullerton et al., 1989; Powell et al., 1988) that the pattern of spreading developed in the Early Cretaceous persisted up to the beginning of the Late Cretaceous (96 my). Powell predicted a position of the spreading ridge, which became extinct at 96 my (Powell et al., 1988). Its axis coincides with a bathymetric high in the southeastern part of the Christmas Island Rise (Fig. 22). The northern part of the Rise trends similarly to the NE, most of the seamounts being slightly elongated in this direction. It is possible that the whole Christmas Island Rise was initially formed as a mid-ocean ridge, which was abandoned 96 my ago. In this case the uplifted block, associated with the Christmas Island Rise, may represent remnants of this spreading ridge.

Late Cretaceous magnetic lineations of the new generation (84-50 my) were identified only in the westernmost part of the studied area. However, we suggest that N-S trending fracture zones observed further to the east (Fig. 18) represent transform faults developed during the period. The age of the crust fractured by these faults therefore should be Late Cretaceous. One of the drilling sites of the Deep Sea Drilling Project (site 211) was located west of Christmas Island ($9^{\circ} 46.53' \text{ S}$, $102^{\circ} 41.95' \text{ E}$). The oldest sediments recovered by the core

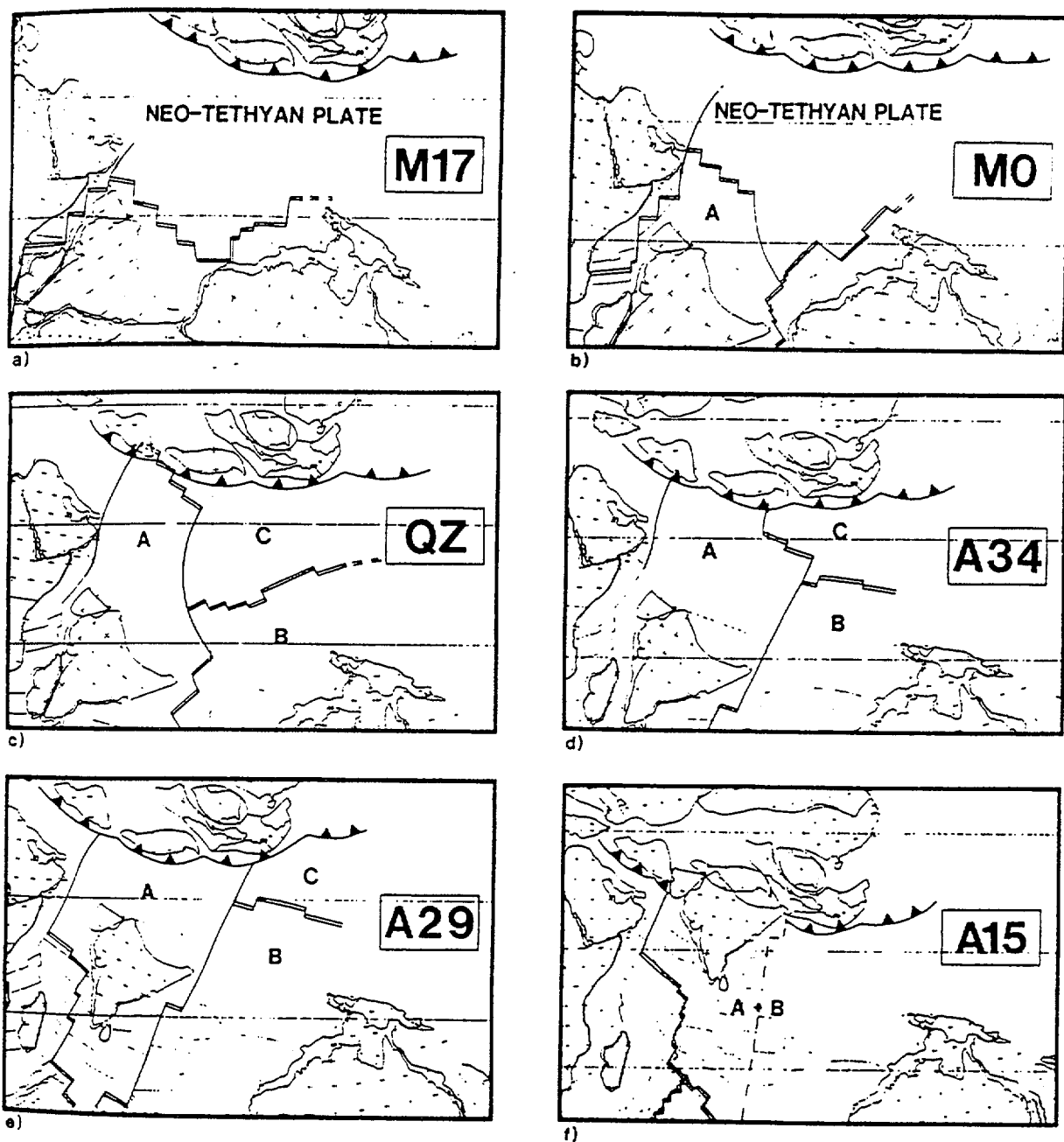


Fig. 23. Hypothetical plate boundaries in the Tethys during Mesozoic and Cenozoic (after Scotese et al., 1988): a) Early Cretaceous; b) Middle Cretaceous; c) Cretaceous Magnetic Quiet Zone; d) Late Cretaceous; e) Paleocene; f) Oligocene.

were Late Campanian (71 my) overlying a dolerite sill of the same age (McDougall, 1974; von der Borch et al., 1972). According to identified magnetic lineations, the displacement along all transform faults east of the Ninetyeast Fracture Zone was left-lateral. Assuming that it was the same in the studied area, we suggest that most of the Late Cretaceous crust in the studied area was formed between the Santonian and Maastrichtian (from 84 to 69 my ago).

Without adequate interpretation of magnetic anomalies or additional drilling, it is very difficult to establish the position of the boundary between the two crustal areas. A proposed position of this boundary is shown in Fig.18. I suggest that it lies immediately to the northwest of the Christmas Island Rise, so almost all seamounts lie within 100-96 my crust. My conclusion is based on the clear evidence that NW fracture zones of the Early Cretaceous system cut through the Christmas Island Rise. They can be traced without interruption for hundreds of kilometres to the east. I have shown the easternmost boundary between the two crustal zones coinciding with a N-S trending fracture zone at about 106°E. Here the basement within the trench deepens abruptly eastward from 7000-7200 m to 7600-7800 m. I consider this is an evidence that crustal age to the east of this fracture zone is considerably greater than to the west of it. If my suggestion is right, and the fracture zone at 106°E really divides crustal areas formed during different episodes of spreading, then the age difference between the adjacent parts of the plate carried into the trench would be not less than 15 my, which explains the trench deepening.

Seamount age and origin

Seamounts in the vicinity of Christmas Island are often considered to be a continuation of Vening-Meinesz seamounts (Exon, 1991; Williams and Exon, 1992). Moreover, it was suggested (Williams, 1992) that the Cocos Keeling Islands, lying to the west of Vening-Meinesz seamounts, may be a continuation of the same seamount chain. All these seamount groups are only superficially studied. Data collected in BMR Cruise 107 gave new insights on the age and origin of the seamounts in the Christmas Island region.

Major element geochemical analysis of seamount lavas (basalts and trachytes) and samples from Christmas Island indicate that both the seamounts and Christmas Island resulted from normal intraplate volcanism. Samples collected from the slopes of the seamounts are represented by shallow water bioclasts of Late Cretaceous age. Foraminiferal and nannofossil biostratigraphy of the samples (Chaproniere and Coleman, 1992, Shafik, 1992) indicate that the seamounts had ceased active volcanism before the Late Cretaceous. By the Maastrichtian, water depths had increased sufficiently to attract pelagic sedimentation. The volcanic igneous content of some of the Late Cretaceous/Maastrichtian samples suggests

limited volcanic activity at this time. Some dredges also recovered Eocene volcanoclastic sediments.

Some constraints on age and origin of the seamounts were obtained from new data on the geology of Christmas Island presented by Falloon et al. (1993). Studies of the Christmas Island lavas showed that there was a reactivation of volcanism in the Eocene (35-40 my ago), when lavas similar to those formed in the Late Cretaceous were produced. Christmas Island rocks display also a very recent, Pliocene, volcanic phase (3-5 my ago). It is postulated that this recent volcanism was caused by fracturing of the lithosphere as it moves towards the Sunda Trench (Falloon et al., 1993).

An interesting observation was made by S. Williams (1992) concerning subsidence rates of the Christmas Island seamounts in comparison to the Vening-Meinesz and Cocos-Keeling groups. All the seamounts in the Christmas Island region have subsided much more slowly than the seamounts lying to the west. This means that either the rate of subsidence was less than that assumed, the volcanoes submerged more recently than assumed, or there was some thermal uplift of the region.

There are three possible tectonic settings in which intraplate volcanism may occur (Williams, 1992): 1) along fracture zones; 2) in the zones of intraplate stress; 3) in the vicinity of a hotspot. It has been suggested that the Vening-Meinesz seamounts have a hotspot origin. Rock geochemistry and the general strike of the seamount chain seem to be consistent with this origin. However, the new bathymetric map compiled later shows that the strike of the Christmas Island Rise differs from that of the Vening-Meinesz seamounts (to the west of 103°E). It has NE-SW orientation consistent with Early Cretaceous magnetic lineations and is fractured by faults normal to its orientation; its position coincides with the predicted position of the 96 my spreading axis. Even the structure of Christmas Island itself shows an obvious trend in this direction (Fig.24). If all the seamounts reflected the trace of a hotspot, then their strike would be unchanged within the Late Cretaceous crust. The change in the hotspot trace may have occurred only after 50 Ma, when the Indian and Australian plates were joined together. Prior to that the Australian plate was mostly rotating clockwise, which is consistent with the trend of the Vening-Meinesz seamounts, but not the Christmas Island rise. After 50 Ma the Indo-Australian plate was moving generally northwards, but the seamounts in the Christmas Island area could not have been formed by a hotspot at this stage, because according to biostratigraphic data, most of them already existed by the Maastrichtian.

Moreover, comparison of different bathymetric swells associated with hotspots (Heestand et al., 1981; Monnereau and Cazenave, 1990; Borissova and Kazmin, 1992), shows that

CHRISTMAS ISLAND

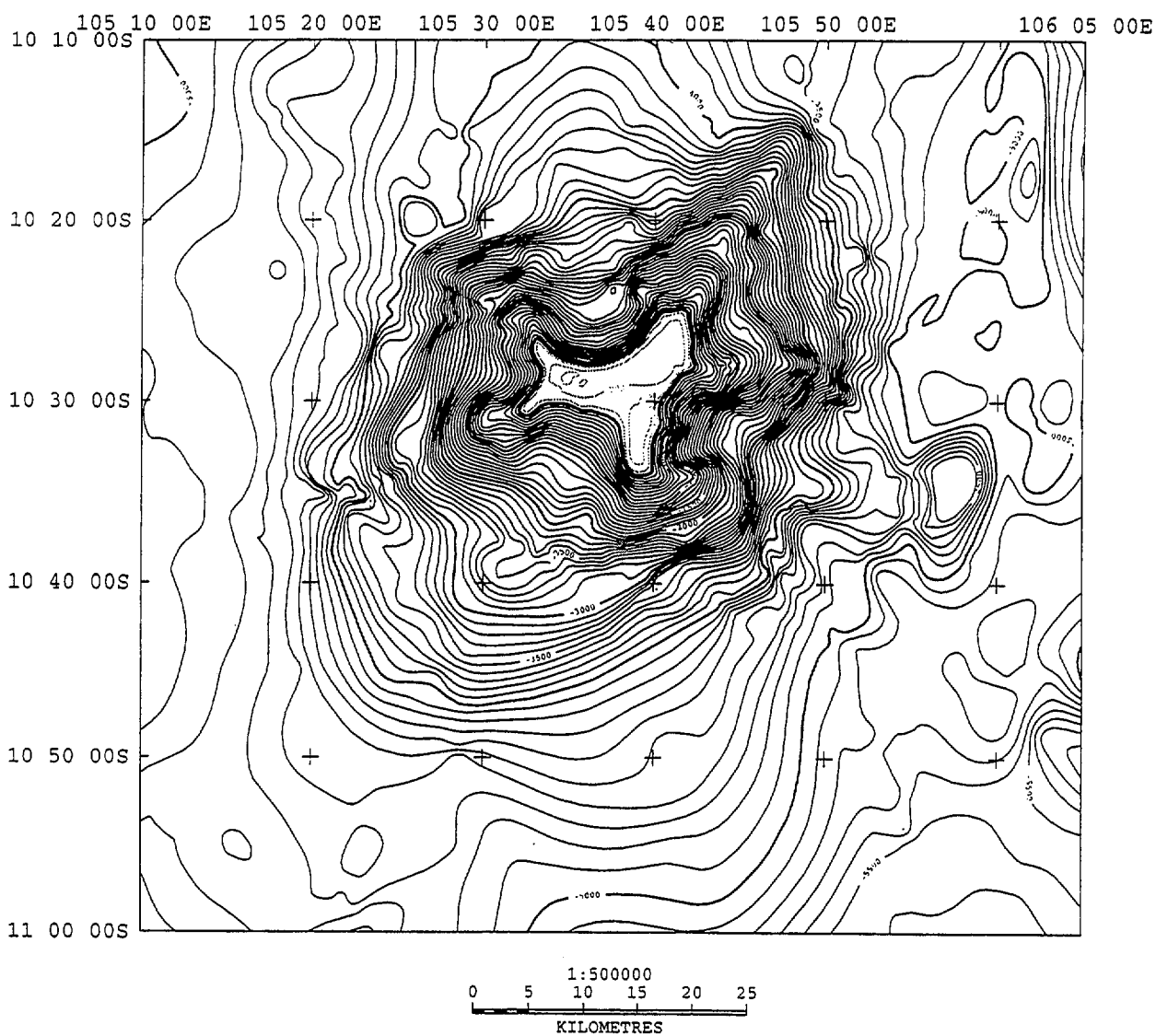


Fig. 24. Detailed bathymetry of Christmas Island.

hotspot traces are surrounded by anomalously shallow areas, hundreds (400-600) of kilometres away from the volcanic centres. The Christmas Island rise is only about 250 km wide. It doesn't look like a swell, because there is an abrupt change from the uplifted area to the deep parts of the basin, where depths are consistent with the crustal age.

We consider that volcanism of the studied seamounts was associated with reactivation of old fracture zones during periods of major plate reorganisation, accompanied by increased intraplate stress. We suggest that high volcanic edifices, some of them emerging above sea level, were formed about 15 my after spreading ceased at the Early Cretaceous spreading ridge (95 Ma). Intensive volcanic activity was associated with a new spreading centre that started to propagate from the west. The new plate boundary was formed very close to the position of the former spreading axis, but the spreading direction changed by almost 45°. It cut off parts of the former spreading ridge and they were carried away to the north. Propagating of the new spreading centre through the old rigid lithosphere caused volcanic activity at places with weakened crust, mostly at the intersections with old fracture zones. A thermal anomaly associated with the extinct spreading ridge contributed to the general elevation of the area and intensity of volcanism. Volcanic activity started about 80 my ago and it may have lasted a few million years, while the new spreading ridge was still close.

The Eocene volcanism in the Christmas Island area follows a very important stage in evolution of the Indian ocean, collision of Greater India with Eurasia and cessation of spreading in the Wharton Basin (50 my), when the Indo-Australian plate started to subside directly beneath Eurasia. The Eocene volcanism may have been caused by intraplate stress associated with those changes.

The most recent volcanic activity on Christmas Island is probably also caused by intraplate stress and reactivation of fracture zones, this time caused by lithospheric flexure developed near the subduction zone.

Conclusions

- The Christmas Island area consists of two dramatically different physiographic and tectonic provinces: Wharton basin province, formed at the end of the Early Cretaceous and the beginning of the Late Cretaceous; and Java province - a modern subduction complex, developed at least since Oligocene.
- Within the studied area, the morphology and structure of the trench and accretionary wedge changes from north-west to south-east. In the west, the trench is shallower and the fore-arc ridge is higher, which is consistent with oblique subduction and shallower dip of the Benioff zone; whereas in the east the trench is

deeper and narrower, corresponding to frontal subduction with steeper dip of the subducting slab.

- The trench and fore-arc ridge structure display irregularities, caused by collision of seamounts with the accretionary wedge. Different stages of seamount collision cause different changes in fore-arc morphology, from collision "scars" and steep crescentic slopes, to local highs on the fore-arc ridge.

- The trench has a segmented structure, consisting of deeps divided by shallow saddles. The boundaries between the segments are associated either with old fracture zones, or with the seamounts carried into the trench.

- The most striking feature of Wharton Basin morphology is the abundance of large seamounts, Late Cretaceous volcanoes, in some cases with evidence of later Eocene volcanism, forming two broad seamount chains trending from SW to NE. The western group of the seamounts, including Christmas Island, is shallower and volcanoes are superimposed on the rise, about 1000 m high. Both the seamount groups are dissected by fracture zones normal to their strike, clearly expressed in bottom topography.

- Structural trends within the Christmas Island rise indicate that it was formed prior to development of the Late Cretaceous-Paleocene spreading system, when spreading directions changed almost 45°. The position and strike of the Christmas Island rise coincides with the predicted position of the spreading centre becoming extinct at 96 Ma. We suggest that the boundary between the two crustal provinces lies immediately to the west of the rise.

- Seamount volcanism in the studied area was associated with reactivation of old transform faults of the extinct spreading centre. Major volcanic activity took place in the Late Cretaceous, about 80 my ago, as the new spreading centre was propagating through the old oceanic crust to the west. The Eocene, second stage of volcanic activity, occurred about 35-40 m.y. ago, soon after the fusion of the Indian and Australian plates, when spreading ceased in the Wharton Basin. The third stage of volcanic activity, about 3-5 m.y. ago, was confined probably only to Christmas Island, and was caused by lithospheric flexure and fault reactivation as the area approached the Java Trench.

REFERENCES

- AUDLEY-CHARLES M.G., BALLANTYNE P.D. AND HALL R., 1988 - Mesozoic-Cenozoic rift-drift sequence of Asian fragments from Gondwanaland. *Tectonophysics*, 155: 317-330.
- BORISSOVA I.A., KAZMIN V.G. - Age-depth relationship in Northern Atlantic and the possible connections with the break-up history of the continents . *Oceanologia*, submitted in 1992.
- BREEN N.A., SILVER E.A. AND HUSSONG D.M., 1986 - Structural styles of an accretionary wedge south of the island of Sumba, Indonesia, revealed by SeaMARC II side scan sonar. *Geol. Soc. Am. Bull.*, 97: 1250-1261.
- CHAPRONIERE G.C. AND COLEMAN P.J., 1992 - Foraminiferal biostratigraphy of dredge samples. In: BMR cruise 107: seabed morphology and offshore resources around Christmas Island, Indian Ocean, AGSO Record 1993/6, 51-59.
- CURRAY J.R., SHOR G.G., RAITT R.W., AND HENRY M., 1977 - Seismic refraction studies of crustal structure of the Eastern Sunda and western Banda arcs. *J. Geophys. Res.*, vol. 82,: 2479-2489.
- DEMETS C., 1992 - Oblique convergence along the Kuril and Japan Trenches. *J. Geophys. Res.*, vol 97-B: 17615-17625.
- EXON N.F., 1991 - Seabed morphology and offshore resources around Christmas Island, Indian Ocean, project 121.32 Research cruise Proposal. BMR Record 1991/92.
- FALLOON T.J., VARNE R., HART S. AND DUNCAN R.A., 1993 - Alkaline rocks from Christmas Island, NW Indian Ocean: a record of northeast Indian Ocean Tertiary magmatism (in press).
- FRYER P. AND SMOOT N.C., 1985 - Processes of seamount subduction in the Mariana and Izu-Bonin trenches. *Mar. Geol.*, 64: 77-90

- FULLERTON L.G., SAGER W.W. AND HANDSCHUMACHER D.W., 1989 - Late Jurassic - Early Cretaceous evolution of the Eastern Indian ocean, adjacent to northwest Australia. *Journal of Geophys. Res.*, 94-B:2937-2953.
- GEIST E.L., CHILDS J.R. AND SCHOLL D.W., 1988 - The origin of summit basins of the Aleutian Ridge: implications for block rotation of an arc massif. *Tectonics*, 7: 327-341.
- HAMILTON W., 1974 - Map of sedimentary basins of the Indonesian region. US Geol. Surv. Misc. Invest. Ser. Map I-875-B.
- HAMILTON W., 1979 - Tectonics of the Indonesian region. US Geol. Survey, Prof. Pap., 1078:345 pp.
- HEESTAND R.L. AND CROUGH S.T., 1981- The effect of hotspots on the oceanic age-depth relation. *J. Geophys. Res.*, 86-B: 6107-6114.
- HUCHON P. AND LE PICHON X., 1984 - Sunda strait and Central Sumatra fault. *Geology*, 12: 668-672.
- KOBAYASHI K. ET AL., 1987 - Normal faulting of the Daiichi-Kashima Seamount in the Japan Trench revealed by the Kaiko 1 cruise, Leg. 3. *Earth and Planetary Science Letters*, 83: 257-266.
- LALLEMAND S. AND LE PICHON X., 1987 - Coulomb wedge model applied to the subduction of seamounts in the Japan Trench. *Geology*, 15: 1065-1069.
- LASSAL O., HUCHON PH. AND HARJONO H., 1989 - Extension crustale dans le detroit de la Sonde (Indonesie). *Donnees de la sismique reflexion (campagne KRAKATAU)*. C.R. Acad. Sci. Paris, 309, ser. II, 205-212.
- LIU C.S., CURRAY J.R. AND MCDONALD J.M., 1983 - New constraints on the tectonic evolution of the Indian Ocean. *Earth. Planet. Sci. Lett.*, 65: 331-342.
- LONSDALE P., 1986 - A multibeam reconnaissance survey of the Tonga trench axis and its intersection with the Louisville Guyot chain. *Marine Geophys. Res.*, 8: 295-327.
- MASSON D.G., PARSON L.M., MILSOM J., NICHOLS G., SIKUMBANG N., DWIYANTO B. AND H. KALLAGHER, 1990 - Subduction of seamounts at the Java Trench: a view with long-range sidescan sonar. *Tectonophysics*, 185: 51-65.
- MCCAFFREY R., 1992 - Oblique plate convergence, slip vectors and forearc deformation. *J. Geophys. Res.*, 97-B: 8905-8915.

MCDUGALL I., 1974 - Potassium-argon ages on basaltic rocks recovered from DSDP Leg. 122, Indian Ocean. In: von der Borch et al.: Initial Reports of the Deep Sea Drilling Project, Washington D.C., 22, 377-379.

MILSOM J., MASSON D. AND NICHOLS G., 1992 - Three trench endings in eastern Indonesia. *Mar. Geol.*, 104: 227-241.

MONNEREAU M. AND CAZENAVE A., 1990 - Depth and Geoid anomalies over oceanic hotspot swells: a global survey. *J. Geophys. Res.*, 95-B: 15429-15438.

MOORE G.F., CURRAY J.R., MOORE D.G. AND KARIG D.E., 1980 - Variations in geologic structure along the Sunda forearc, northeastern Indian ocean. In: D.E. Hayes (Editor), *Tectonic and Geologic Evolution of the Southeastern Asian Seas and Islands*. *Geophys. Monograph.*, AGU, 23: 145-160.

NEWCOMB K.R. AND MCCANN W.R. 1987 - Seismic history and seismotectonics of the Sunda arc. *Journal of Geophysical Research*, 92-B: 421-439.

PATRIAT P. AND ACHACHE J., 1984 - India-Eurasia collision chronology has implications for crustal shortening and driving mechanisms of plates. *Nature*, 311: 615-621.

POWELL C. MC.A., ROOTS S.R. AND VEEVERS J.J., 1988 - Pre-breakup continental extension in East Gondwanaland and the early opening of the eastern Indian Ocean. *Tectonophysics*, 155: 261-284.

SCHOLL D.W., VALLIER T.L. AND STEVENSON A.J., 1982 - Sedimentation and deformation in the Amlia Fracture zone section of the Aleutian Trench. *Mar. Geol.*, 48:105-134.

SCOTese C.R., GAHAGAN L.M. AND LARSON R.L., 1988 - Plate tectonic reconstructions of the Cretaceous and Cenozoic ocean basins. *Tectonophysics*, 155: 27-48.

SENO T. AND EGUCHI T. 1983 - Seismotectonics of the western Pacific region. In: T.W.C. Hilde and S. Uyeda (Editors) *Geodynamics of the Western Pacific-Indonesian Region*. AGU, *Geodyn. Ser.*, 11: 5-40.

SHAFIK S., 1992 - Calcareous nannofossil biostratigraphy of rocks dredged from seamounts near Christmas Island. In: BMR cruise 107: seabed morphology and offshore resources around Christmas Island, Indian Ocean, AGSO Record 1993/6, 60-70.

Tectonic map of the Circum-Pacific Region. Southwest quadrant., 1991.

VEEVERS J.J. AND LI Z.X., 1991 - Review of seafloor spreading around Australia. II. Marine magnetic anomaly modelling. *Austr. J. Earth Sci.*, 38: 391-408.

VON DER BORCH C.C. & SCLATER J.G. ET AL., 1974 - Initial Reports of the Deep Sea Drilling Project, 22, Washington, US Govt Printing Office, 13-21.

WILLIAMS S.M. AND EXON N.F., 1992 - Rocks and sediments dredged from seamounts. In: BMR cruise 107: seabed morphology and offshore resources around Christmas Island, Indian Ocean, AGSO Record 1993/6, 29-38.

WILLIAMS S.M., 1992 - Origin and subsidence history of seamounts in the Christmas Island offshore region, Indian Ocean. Honours thesis, ANU Geology Dept., 67 pp.